



Neurobehavioural characterisation and stratification of reinforcement-related behaviour

Tianye Jia ^{1,2,3,4} ✉, Alex Ing³, Erin Burke Quinlan ³, Nicole Tay ³, Qiang Luo ^{1,2,3,4,5}, Biondo Francesca ⁵, Tobias Banaschewski ⁶, Gareth J. Barker ⁷, Arun L. W. Bokde⁸, Uli Bromberg⁹, Christian Büchel ⁹, Sylvane Desrivières ³, Jianfeng Feng^{1,2,3,10,11,12,13}, Herta Flor^{14,15}, Antoine Grigis¹⁶, Hugh Garavan¹⁷, Penny Gowland¹⁸, Andreas Heinz¹⁹, Bernd Ittermann²⁰, Jean-Luc Martinot ^{21,22}, Marie-Laure Paillère Martinot ^{21,23}, Frauke Nees^{6,14}, Dimitri Papadopoulos Orfanos ¹⁶, Tomáš Paus²⁴, Luise Poustka²⁵, Juliane H. Fröhner ²⁶, Michael N. Smolka ²⁶, Henrik Walter ¹⁹, Robert Whelan ²⁷, Gunter Schumann ^{1,3,28} ✉ and IMAGEN Consortium*

Reinforcement-related cognitive processes, such as reward processing, inhibitory control and social-emotional regulation are critical components of externalising and internalising behaviours. It is unclear to what extent the deficit in each of these processes contributes to individual behavioural symptoms, how their neural substrates give rise to distinct behavioural outcomes and whether neural activation profiles across different reinforcement-related processes might differentiate individual behaviours. We created a statistical framework that enabled us to directly compare functional brain activation during reward anticipation, motor inhibition and viewing emotional faces in the European IMAGEN cohort of 2,000 14-year-old adolescents. We observe significant correlations and modulation of reward anticipation and motor inhibition networks in hyperactivity, impulsivity, inattentive behaviour and conduct symptoms, and we describe neural signatures across cognitive tasks that differentiate these behaviours. We thus characterise shared and distinct functional brain activation patterns underlying different externalising symptoms and identify neural stratification markers, while accounting for clinically observed comorbidity.

Reinforcement-related behaviours are commonly implicated in normal behaviour and psychopathology. Symptoms of dysfunctional reinforcement-related cognitive processes may present as hyperactivity, inattention, and conduct and emotional problems¹. These symptoms are manifest in common psychiatric disorders, such as depression, attention-deficit/

hyperactivity disorder (ADHD), addictions, conduct disorder and psychosis^{2,3}, and share similar reinforcement-related cognitive processes, including reward processing, inhibitory control and social-emotional regulation⁴. However, while similar cognitive processing deficits are involved in different disorders, there are clear differences in their behavioural presentation in each disorder.

¹Centre for Population Neuroscience and Precision Medicine (PONS), Institute of Science and Technology for Brain-Inspired Intelligence, Fudan University, Shanghai, China. ²MoE Key Laboratory of Computational Neuroscience and Brain-Inspired Intelligence, Fudan University, Shanghai, China. ³Centre for Population Neuroscience and Precision Medicine (PONS), Institute of Psychiatry, Psychology & Neuroscience, SGDP Centre, King's College London, London, UK. ⁴MOE Frontiers Center for Brain Science, Institutes of Brain Science, Fudan University, Shanghai, China. ⁵State Key Laboratory of Medical Neurobiology, Fudan University, Shanghai, China. ⁶Department of Child and Adolescent Psychiatry and Psychotherapy, Central Institute of Mental Health, Medical Faculty Mannheim, Heidelberg University, Mannheim, Germany. ⁷Department of Neuroimaging, Institute of Psychiatry, Psychology & Neuroscience, King's College London, London, UK. ⁸Discipline of Psychiatry, School of Medicine and Trinity College Institute of Neuroscience, Trinity College Dublin, Dublin, Ireland. ⁹University Medical Centre Hamburg-Eppendorf, Hamburg, Germany. ¹⁰Institute for Science and Technology of Brain-inspired Intelligence (ISTBI), Fudan University, Shanghai, P.R. China. ¹¹Department of Computer Science, University of Warwick, Coventry, UK. ¹²Collaborative Innovation Center for Brain Science, Fudan University, Shanghai, PR China. ¹³Shanghai Center for Mathematical Sciences, Shanghai, PR China. ¹⁴Institute of Cognitive and Clinical Neuroscience, Central Institute of Mental Health, Medical Faculty Mannheim, Heidelberg University, Mannheim, Germany. ¹⁵Department of Psychology, School of Social Sciences, University of Mannheim, Mannheim, Germany. ¹⁶NeuroSpin, CEA, Université Paris-Saclay, Gif-sur-Yvette, France. ¹⁷Departments of Psychiatry and Psychology, University of Vermont, Burlington, Vermont, USA. ¹⁸Sir Peter Mansfield Imaging Centre School of Physics and Astronomy, University of Nottingham, University Park, Nottingham, UK. ¹⁹Department of Psychiatry and Psychotherapy CCM, Charité – Universitätsmedizin Berlin, corporate member of Freie Universität Berlin, Humboldt-Universität zu Berlin, and Berlin Institute of Health, Berlin, Germany. ²⁰Physikalisch-Technische Bundesanstalt (PTB), Braunschweig and Berlin, Brunswick, Germany. ²¹Institut National de la Santé et de la Recherche Médicale, INSERM Unit 1000 “Neuroimaging & Psychiatry”, University Paris Saclay, University Paris Descartes; Dlgiteo-Labs, Gif-sur-Yvette, France. ²²Maison de Solenn, Paris, France. ²³AP-HP.Sorbonne Université, Department of Child and Adolescent Psychiatry, Pitié-Salpêtrière Hospital, Paris, France. ²⁴Bloorview Research Institute, Holland Bloorview Kids Rehabilitation Hospital and Departments of Psychology and Psychiatry, University of Toronto, Toronto, Ontario, Canada. ²⁵Department of Child and Adolescent Psychiatry and Psychotherapy, University Medical Centre Göttingen, Göttingen, Germany. ²⁶Department of Psychiatry and Neuroimaging Center, Technische Universität Dresden, Dresden, Germany. ²⁷School of Psychology and Global Brain Health Institute, Trinity College Dublin, Dublin, Ireland. ²⁸PONS Research Group, Dept of Psychiatry and Psychotherapy, Campus Charité Mitte, Humboldt University, Berlin, Germany. *A list of authors appears at the end of the paper. ✉e-mail: tianyejia@fudan.edu.cn; gunter.schumann@kcl.ac.uk

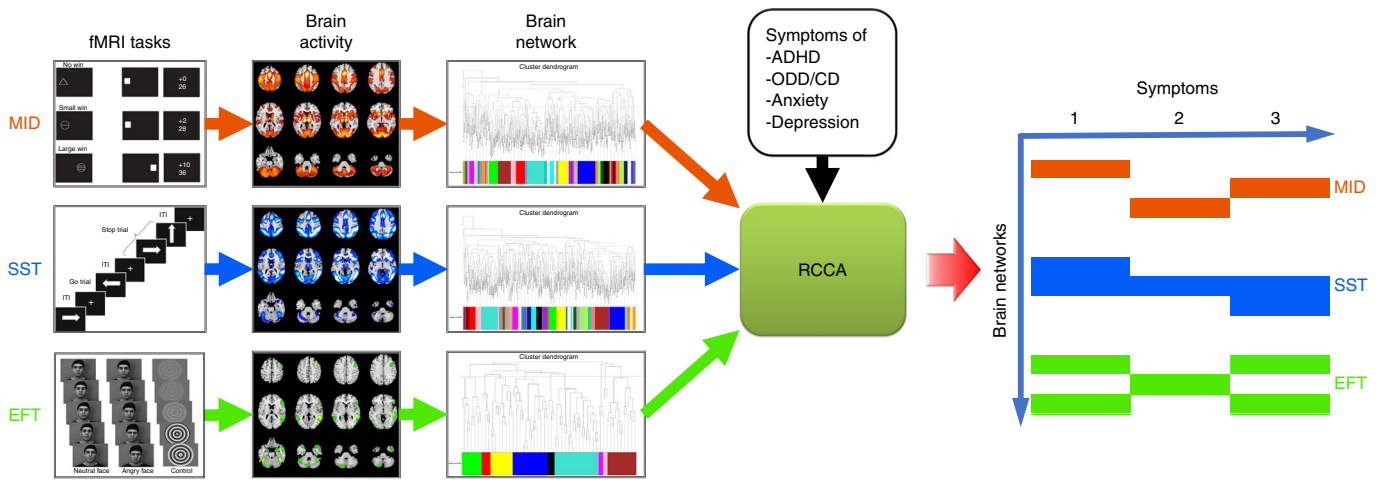


Fig. 1 | Workflow of the analyses. We included the MID task⁶ as a measure of reward processing, the SST⁵² as a measure of impulsivity (motor inhibition) and the EFT²² as a measure of social-emotional processing, for which the figures of experimental models were adapted from previous publications^{6,22,52}. Only strong brain activation (effect size: Cohen’s $D > 0.30$) was included in the analyses. The WVCNA, in combination with a further hierarchical clustering, was implemented to establish the brain fMRI networks. The RCCA was adopted to evaluate the overall correlation between the brain networks and reinforcement-related behaviours. Based on the RCCA results, we identified the neural signatures across three brain fMRI networks for each reinforcement-related behaviour. ITI, intertrial interval.

It is unclear whether and how the reinforcement-related cognitive processes are modulated to achieve the observed behavioural differences among these disorders. Identifying the brain activity patterns related to various manifestations of dysfunctional reinforcement-related behaviour might aid in the characterization of underlying biological mechanisms, and in the identification of targets for therapeutic intervention⁵. Furthermore, clinically relevant psychiatric symptoms are typically characterized by dysfunctions not only in one but often in several reinforcement-related cognitive processes. For example, ADHD symptoms are known to involve dysfunctional inhibitory control¹, as well as dysfunctional reward processing⁶. We were interested in dissecting the contribution of different domains of reinforcement-related cognitive processes to distinct disorder symptoms, and thus characterizing a profile of brain activation specific for each disorder.

Whereas animal models have identified networks of multiple cortical and subcortical brain regions involved in reinforcement-related cognitive processes⁷, analyses in humans are often based on a few predefined regions of interest (ROIs). These include the ventral striatum and orbitofrontal cortex (OFC) for reward processing⁸, the right inferior frontal cortex (rIFC) for inhibitory control⁹ and the amygdala and superior temporal sulcus (STS) for social-emotional regulation^{10,11}. Often, the underlying assumption is that a cognitive process can be represented by a few key brain regions. However, we¹² and others^{13–16} have shown that task-induced brain activity may involve a complex network of cortical and subcortical brain regions. What we do not know is how activity in these networks relates to observable behaviour.

In this paper, we provide a systematic characterization of brain activity in reinforcement-related behaviour, measuring blood oxygen level-dependent (BOLD) response during tasks targeting reward anticipation, motor inhibition and social-emotional processing. We compare their common and distinct brain activity patterns and assess the modulation of task-specific networks in externalizing (for example, hyperactivity, inattention, impulsivity and conduct symptoms) and internalizing behavioural symptoms (for example, emotional and anxiety symptoms)¹⁷. We also identify signatures of brain activity across tasks that best characterize symptoms of externalizing disorders, as well as helping to distinguish one symptom domain from the other.

Results

Summary of the analysis strategy. We aimed to compare brain activity during functional neuroimaging tasks measuring reward anticipation, motor inhibition and social-emotional processing of 1,506 14-year-old adolescents from the IMAGEN (reinforcement-related behaviour in normal brain function and psychopathology) project⁴. Of the 1,506 participants investigated in this study, clinical development and well-being assessment (DAWBA) ratings were available from 1,190 individuals. Of these individuals, 131 had one or more diagnoses; 33 individuals were diagnosed with ADHD, 59 with emotional problems, 12 with anxiety (general + other) and 33 with depression (major + other). We reduced the dimensionality of brain activation by applying a weighted voxel co-activation network analysis (WVCNA)^{12,18}, followed by a hierarchical clustering analysis. The combination of both methods could efficiently reduce dimensionality while still preserving localized network features from WVCNA. We then calculated the overall correlation between functional MRI (fMRI) clusters and symptoms of externalizing or internalizing behaviours using ridge-regularized canonical correlation analysis (RCCA)¹⁹—a method to detect multivariate relationships between different data types.

First, we tested for an overall significant correlation of externalizing or internalizing symptoms with brain network activation across all fMRI tasks. In cases where we established an overall correlation, we looked for associations of each fMRI network with externalizing or internalizing behaviours. Finally, we investigated the sensitivity and specificity of fMRI clusters across different behaviour components. This workflow is shown in Fig. 1.

Identification of reinforcement-related brain fMRI networks. We defined brain networks underlying reinforcement-related behaviour by using the monetary incentive delay (MID) task to measure reward processing²⁰, the stop signal task (SST) to assess motor inhibition²¹ and the emotional faces task (EFT) to examine social-emotional processing²². In these tasks, we analysed contrasts that were most relevant to the reinforcement-related behaviour and eliciting the largest BOLD difference; namely, the large win versus no win contrast during the reward anticipation phase in the MID task, the successful stop versus successful go contrast in the SST, and the angry face versus control contrast in the EFT.

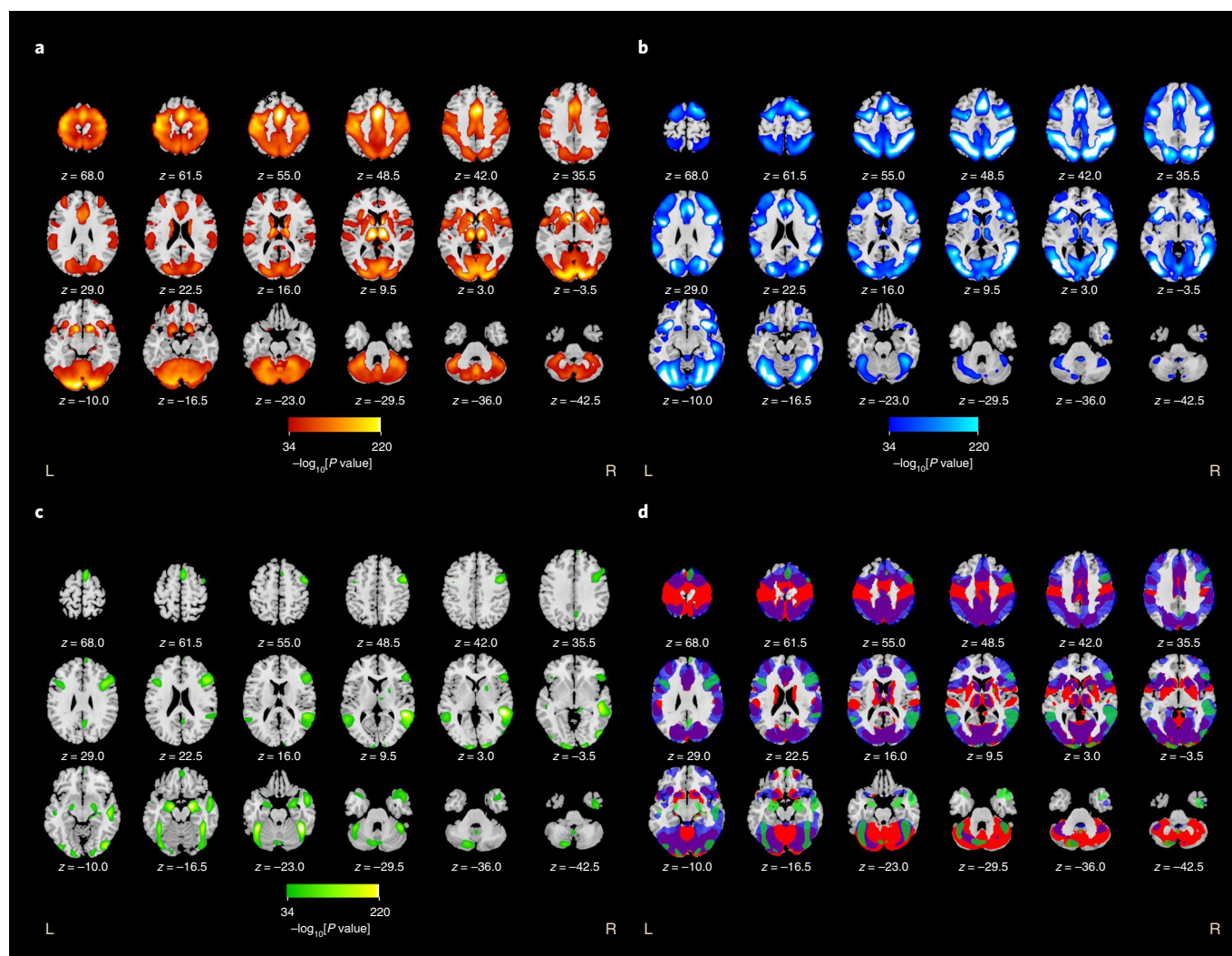


Fig. 2 | Activation maps of MID, SST, EFT and their overlay. **a–d**, Activation maps showing activation for a large win versus no win in the MID task (**a**), successful stop versus successful go in the SST (**b**), the angry face versus the control face in the EFT (**c**) and overlay of the results for all three tasks (**d**). MID, SST and EFT are represented by red, blue and green, respectively. Activation levels were measured as the $-\log_{10}(\text{transformed } P \text{ value})$ and only voxels with $P < 1.0 \times 10^{-34}$ (that is, Cohen's $D > 0.3$) are shown. L, left; R, right.

We applied WVCNA^{12,18}, which was established by combining the scale-free network assumption with a dynamic cut of the dendrogram²³, to maximize the resolution of localized brain network features (see Methods for details). Using this approach, we identified in the MID a brain network consisting of 500 nodes (25,130 voxels; Fig. 2a), 487 nodes (24,571 voxels) in the SST (Fig. 2b) and 79 nodes (3,923 voxels) in the EFT (Fig. 2c). We further removed redundant information by applying an additional hierarchical clustering on these nodes with a static cut at the 90th percentile, keeping the 10% most distinctive branches (representing clusters) in each dendrogram. This two-step procedure enabled us to efficiently reduce dimensionality while still preserving localized network features from WVCNA (Supplementary Table 1a–c). Using this approach, we identified 46 clusters in MID, 41 clusters in SST and nine clusters in EFT (Supplementary Table 1a–c and Extended Data Fig. 1).

In all three networks, activated clusters were widely spread across cortical and subcortical regions, as well as in the cerebellum (Fig. 2 and Extended Data Fig. 2). Brain regions activated in the three networks were often overlapping (Fig. 2d). It is notable that none of the ROIs typically associated with reward processing, impulsiveness or social-emotional processing was specific to their corresponding

networks. For example, the ventral striatum and OFC (which are typically linked to reward processing⁸) were activated in both the MID task and the SST, whereas the rIFC (which is often associated with inhibitory control⁹) was activated in both the SST and EFT. The STS, which is regarded as an essential component of the social brain¹¹, was also activated in both the SST and EFT. The dorsal amygdala (a central node of emotional processing¹⁰) was activated not only in the EFT but also in the MID task. However, some activations were network specific. For example, distinct activations were seen in the superior post-central gyrus (that is, the superior primary somatosensory cortex), primary auditory cortex (PAC), dorsal striatum and most of the cerebellar vermis during the MID task, in the frontal operculum, the orbital part of the rIFC, the inferior primary somatosensory cortex and the lingual part of the cerebellar vermis during the SST, and in the medial OFC, dorsal posterior cingulate cortex, temporal pole and ventral amygdala during the EFT (Fig. 2d and Extended Data Fig. 2).

Modulation of reinforcement-related brain fMRI networks in different behaviours. Clinical psychopathology in adolescents is grouped into externalizing and internalizing disorders²⁴. We were interested in examining whether externalizing and internalizing

Table 1 | List of externalizing items from the parent-rated SDQ and DAWBA and internalizing items from the child-rated SDQ and DAWBA

Externalizing items from the parent-rated SDQ and DAWBA
Hyperactivity
Restless (SDQ_Parent)
Fidgety (SDQ_Parent)
Adhd.fidgets (DAWBA_Parent).
Adhd.cant.remain.seated (DAWBA_Parent)
Adhd.runs.or.climbs.when.shouldnt (DAWBA_Parent)
Adhd.cant.play.quietly (DAWBA_Parent)
Adhd.cant.calm.down (DAWBA_Parent)
Inattention
Easily Distracted (SDQ_Parent)
Attentiveness (SDQ_Parent)
Adhd.careless.mistakes.inattentive (DAWBA_Parent)
Adhd.loses.interest (DAWBA_Parent)
Adhd.doesnt.listen (DAWBA_Parent)
Adhd.doesnt.finish (DAWBA_Parent)
Adhd.poor.self.organisation (DAWBA_Parent)
Adhd.avoids.tasks.needing.thought (DAWBA_Parent)
Adhd.loses.things (DAWBA_Parent)
Adhd.distractible (DAWBA_Parent)
Adhd.forgetful (DAWBA_Parent)
Impulsivity
Think before action (SDQ_Parent)
Adhd.blurts.out.answers (DAWBA_Parent).
Adhd.cant.wait.for.a.turn (DAWBA_Parent)
Adhd.butts.into.conversations.or.games (DAWBA_Parent)
Adhd.unstoppable.talk (DAWBA_Parent)
ODD
Tantrum (SDQ_Parent)
Generally obedient (SDQ_Parent)
Odd.temper.outbursts.parent1 (DAWBA_Parent)
Odd.argues.with.adults.parent1 (DAWBA_Parent)
Odd.ignores.rules.disobedient (DAWBA_Parent)
Odd.deliberately.annoys.others (DAWBA_Parent)
Odd.blames.others.for.own.acts (DAWBA_Parent)
Odd.easily.annoyed (DAWBA_Parent)
Odd.angry.and.resentful (DAWBA_Parent)
Odd.spiteful (DAWBA_Parent)
Odd.vindictive (DAWBA_Parent)
CD
Fight or bully others (SDQ_Parent)
Often lie (SDQ_Parent)
Steal (SDQ_Parent)
Cd.lies (DAWBA_Parent)
Cd.fights (DAWBA_Parent)
Cd.bullies (DAWBA_Parent)
Cd.stays.out (DAWBA_Parent)
Cd.steals (DAWBA_Parent)

Continued

Table 1 | List of externalizing items from the parent-rated SDQ and DAWBA and internalizing items from the child-rated SDQ and DAWBA (Continued)

Externalizing items from the parent-rated SDQ and DAWBA
Cd.runs.away (DAWBA_Parent)
Cd.cannot.find.at.school (DAWBA_Parent)
Internalizing items from the child-rated SDQ and DAWBA
Anxiety
Sepa.any.concerns.about.separations (DAWBA_Self)
Soph.any.concerns (DAWBA_Self)
Panic.attacks.in.last.4.weeks (DAWBA_Self)
Fear.or.avoidance.of.crowds (DAWBA_Self)
Fear.or.avoidance.of.public.places (DAWBA_Self)
Fear.or.avoidance.of.travelling.alone (DAWBA_Self)
Fear.or.avoidance.of.being.far.from.home (DAWBA_Self)
Gena.ever.worries (DAWBA_Self)
Gena.specific.or.generalized (DAWBA_Self)
Gena.excessive.worry (DAWBA_Self)
Many worries (SDQ_Self)
Many fears (SDQ_Self)
Anxious in new situations (SDQ_Self)
Depression
Dep.sad (DAWBA_Self)
Dep.irritable (DAWBA_Self)
Dep.loss.of.interest (DAWBA_Self)
Dep.recent.talk.of.dsh (DAWBA_Self)
Dep.dsh.recently (DAWBA_Self)
Dep.dsh.ever (DAWBA_Self)
Headache/stomach ache (SDQ_Self)
Unhappy (SDQ_Self)

behavioural symptoms correlate with distinct configurations of reinforcement-related networks. From the strength and difficulties questionnaire (SDQ) and DAWBA, we selected the entry-level questions, including 44 externalizing items covering symptoms of ADHD (23 items), oppositional defiant disorder (ODD; 11 items) and conduct disorder (CD; ten items), and 21 internalizing items covering symptoms of depression (12 items) and anxiety (8 items) (Table 1; see Methods for more details). To evaluate the overall relationship between behavioural symptoms and patterns of brain activation, we carried out RCCA¹⁹. This method seeks to find subsets of variables in two datasets that best correlate with each other while stabilizing the result through penalization of correlations within each dataset. We first investigated the overall correlation between externalizing behaviours and 96 clusters from the three fMRI networks and found a significant canonical correlation ($\eta^2 = 0.854$ denotes the proportion of behaviour variance explained by the fMRI and is analogue to R^2 in the multiple linear regression model; 90% confidence interval (CI) = 0.839 to 0.869; adjusted $\eta^2 = 0.160$; d.f._{fMRI} = (1,506, 96); d.f._{behaviour} = (1,506, 44); permutation test P value (P_{perm}) < 0.001; see Methods (for details), Table 2 and Supplementary Table 2). Please note that a predefined scheme of regulation parameters was evaluated throughout for all RCCAs and highly stable results were obtained (as shown in Extended Data Fig. 3). For simplicity, we only show the results with a regulation parameter of 0.1 in the main text. The number of permutations to calculate P values in this

Table 2 | RCCA P values based on 10,000 permutations with penalty $\lambda = 0.1$ for both fMRI and externalizing behaviour items

	ADHD		ODD/CD		All behaviours	
	P value	η^2 (90% CI)	P value	η^2 (90% CI)	P value	η^2 (90% CI)
MID	0.029	0.356 (0.328 to 0.385)	0.203	0.331 (0.301 to 0.361)	0.036	0.565 (0.530 to 0.587)
SST	0.003	0.344 (0.314 to 0.374)	0.003	0.334 (0.303 to 0.366)	<0.001	0.558 (0.530 to 0.587)
EFT	0.634	0.087 (0.067 to 0.108)	0.294	0.091 (0.071 to 0.110)	0.392	0.171 (0.145 to 0.197)
All fMRI					<0.001	0.836 (0.820 to 0.851)

Similar results were achieved with a predefined scheme of penalty settings, as shown in Extended Data Fig. 3. η^2 denotes the proportion of behaviour variance explained by the fMRI and is analogue to R^2 in the multiple linear regression model.

and all subsequent analyses was 10,000 unless otherwise specified. Also, presented P values were always corrected for experiment-wise multiple comparisons wherever applicable. We then investigated the RCCA between internalizing behaviours and the same 96 fMRI clusters, but found no overall significance ($\eta^2 = 0.574$; 90% CI = 0.547 to 0.602); adjusted $\eta^2 = -0.024$; d.f._{fMRI} = (1,506, 96); d.f._{behaviour} = (1506,20); $P_{\text{perm}} = 0.786$; see Extended Data Fig. 4 for more results with alternative parameters). We also did not find significant overall correlations with internalizing behaviours when analysing each fMRI network separately (Extended Data Fig. 4). We therefore constrained our subsequent analyses to externalizing behaviours only.

Next, we investigated the contribution of each brain network to different behavioural conditions. For the reward anticipation network, we found an overall significant correlation with externalizing behaviours ($\eta^2 = 0.579$; 90% CI = 0.551 to 0.607; adjusted $\eta^2 = 0.052$; d.f._{fMRI} = (1,506, 46); d.f._{behaviour} = (1,506, 44); $P_{\text{perm}} = 0.036$; Table 2 and Supplementary Table 2). There was also a significant correlation between reward anticipation and ADHD behaviours ($\eta^2 = 0.365$; 90% CI = 0.335 to 0.394; adjusted $\eta^2 = 0.038$; d.f._{fMRI} = (1,506, 46); d.f._{behaviour} = (1,506, 23); $P_{\text{perm}} = 0.029$; Table 2 and Supplementary Table 2), but not ODD/CD behaviours ($\eta^2 = 0.338$; 90% CI = 0.307 to 0.370; adjusted $\eta^2 = 0.017$; d.f._{fMRI} = (1,506, 46); d.f._{behaviour} = (1,506, 21); $P_{\text{perm}} = 0.203$; Table 2 and Supplementary Table 2), indicating that reward anticipation might be important for ADHD symptoms. For the motor inhibition network, we found an overall significant correlation with externalizing behaviours ($\eta^2 = 0.573$; 90% CI = 0.543 to 0.603; adjusted $\eta^2 = 0.103$; d.f._{fMRI} = (1,506, 41); d.f._{behaviour} = (1,506, 44); $P_{\text{perm}} < 0.001$; Table 2 and Supplementary Table 2). There was also a significant correlation between motor inhibition and ADHD behaviours ($\eta^2 = 0.352$; 90% CI = 0.320 to 0.384; adjusted $\eta^2 = 0.052$; d.f._{fMRI} = (1,506, 41); d.f._{behaviour} = (1,506, 23); $P_{\text{perm}} = 0.003$; Table 2 and Supplementary Table 2) and between motor inhibition and ODD/CD behaviours ($\eta^2 = 0.343$; 90% CI = 0.309 to 0.376; adjusted $\eta^2 = 0.054$; d.f._{fMRI} = (1,506, 41); d.f._{behaviour} = (1,506, 21); $P_{\text{perm}} = 0.003$; Table 2 and Supplementary Table 2), indicating that motor inhibition might play a role in both ADHD and ODD/CD symptoms. For the social-emotional processing network, we found neither significant correlation with externalizing behaviours ($\eta^2 = 0.175$; 90% CI = 0.148 to 0.203; adjusted $\eta^2 = 0.005$; d.f._{fMRI} = (1,506, 9); d.f._{behaviour} = (1,506, 44); $P_{\text{perm}} = 0.392$; Table 2 and Supplementary Table 2), nor with ADHD behaviours ($\eta^2 = 0.089$; 90% CI = 0.068 to 0.110; adjusted $\eta^2 = -0.004$; d.f._{fMRI} = (1,506, 9); d.f._{behaviour} = (1,506, 23); $P_{\text{perm}} = 0.634$; Table 2 and Supplementary Table 2) nor ODD/CD behaviours alone ($\eta^2 = 0.092$; 90% CI = 0.071 to 0.112; adjusted $\eta^2 = 0.004$; d.f._{fMRI} = (1,506, 9); d.f._{behaviour} = (1,506, 21); $P_{\text{perm}} = 0.294$; Table 2 and Supplementary Table 2). While the above RCCA results

provide no indication on the direction of correlation, brain activations during reward anticipation (the MID task) and motor inhibition (the SST) showed predominantly negative correlations with externalizing behaviours through univariate correlation analyses, as shown below (see Table 3 and Supplementary Tables 2–4).

Functional brain characterization of behaviours across different tasks. While both reward anticipation and motor inhibition networks showed significant canonical correlations with ADHD behaviours, neither correlation between the first components of the RCCA (its square is known as Roy's largest root (R_{Roy})²⁵) was significant on its own (reward anticipation: $R_{\text{Roy}} = 0.234$; Fisher R -to- Z transformed correlation (Z_{Fisher}) = 0.237; 90% CI for $Z_{\text{Fisher}} = 0.202$ to 0.274; $P_{\text{perm}} = 0.087$; motor inhibition: $R_{\text{Roy}} = 0.225$; $Z_{\text{Fisher}} = 0.229$; 90% CI for $Z_{\text{Fisher}} = 0.193$ to 0.266; $P_{\text{perm}} = 0.151$), and these correlations were additionally shown to be significantly smaller than a meaningful effect through an equivalence test for inferiority²⁶ (reward anticipation: $t = -3.98$ and $P < 0.001$ for an upper equivalence bound (Z_U) of 0.324; motor inhibition: $t = -4.06$ and $P < 0.001$ for $Z_U = 0.319$; lower equivalence bound (Z_L) = $-\infty$; Z_U was calculated as the estimated inflation of Z_{Fisher} plus a small effect size $\Delta Z = 0.1$ (ref. 27); see Methods for details). These results therefore showed that the overall significant correlation was unlikely to be represented by an individual RCCA component. Therefore, we hypothesized that distinctive neural bases may underlie different ADHD behaviours and investigated profiles across brain networks that may characterize the ADHD components hyperactivity, inattention or impulsivity (see Methods). As the factors generated by RCCA are not optimized to detect differences in the brain function underlying these behaviours, we applied a more sensitive multiple linear regression model. Together, reward anticipation and motor inhibition networks were found in significant association with the summed score (that is, the total score) of ADHD behaviours ($R^2 = 0.085$; 90% CI = 0.063 to 0.106; adjusted $R^2 = 0.029$; $F_{(87, 1,418)} = 1.51$; $P = 0.002$; where R^2 is the coefficient of determinant that represents the proportion of behavioural variance explained by the fMRI networks in the multiple linear model), as well as the total scores of the ADHD components hyperactivity ($R^2 = 0.089$; 90% CI = 0.067 to 0.110; adjusted $R^2 = 0.033$; $F_{(87, 1,418)} = 1.58$; $P < 0.001$), impulsivity ($R^2 = 0.077$; 90% CI = 0.057 to 0.098; adjusted $R^2 = 0.021$; $F_{(87, 1,418)} = 1.37$; $P = 0.017$) and inattention ($R^2 = 0.079$; 90% CI = 0.058 to 0.100; adjusted $R^2 = 0.022$; $F_{(87, 1,418)} = 1.40$; $P = 0.011$). However, we did not find evidence for identical associations of these ADHD behaviours with reward anticipation and motor inhibition networks: while the motor inhibition network was found in significant association with the total scores of all three ADHD components (hyperactivity: $R^2 = 0.045$; 90% CI = 0.028 to 0.061; adjusted $R^2 = 0.018$; $F_{(41, 1,464)} = 1.67$;

Table 3 | Prominent clusters of brain networks for hyperactivity, impulsivity, inattention and ODD/CD behaviours

Hyperactivity								
MID region	Primary behaviour		Exploratory analyses					
	Hyperactivity		Impulsivity		Inattention		ODD/CD	
	R (95% CI)	<i>P</i> _{corrected} (t statistic)	R (95% CI)	<i>P</i> ^a (t statistic)	R (95% CI)	<i>P</i> ^a (t statistic)	R (95% CI)	<i>P</i> ^a (t statistic)
Thalamus	-0.091 (-0.141 to -0.041)	0.011 (-3.539)	-0.032 (-0.089 to 0.012)	0.726 (-1.511)	-0.074 (-0.125 to -0.025)	0.040 (-2.918)	-0.065 (-0.109 to -0.008)	0.118 (-2.276)
SFJ	-0.084 (-0.134 to -0.033)	0.029 (-3.255)	-0.014 (-0.073 to 0.028)	0.992 (-0.873)	-0.066 (-0.117 to -0.016)	0.105 [-2.584]	-0.052 (-0.073 to 0.028)	0.332 [-1.975]
PAC	-0.085 (-0.135 to -0.035)	0.025 (-3.309)	-0.025 (-0.088 to 0.013)	0.771 (-1.442)	-0.051 (-0.098 to 0.002)	0.445 (-1.871)	-0.063 (-0.110 to -0.010)	0.134 (-2.340)
SPL	-0.094 (-0.144 to -0.044)	0.007 (-3.666)	-0.045 (-0.103 to -0.002)	0.324 (-2.055)	-0.077 (-0.127 to -0.027)	0.031 (-3.000)	-0.068 (-0.113 to -0.012)	0.091 (-2.436)
Mid-CS	-0.091 (-0.141 to -0.041)	0.011 (-3.552)	-0.040 (-0.098 to -0.003)	0.452 (-1.860)	-0.075 (-0.124 to -0.024)	0.044 (-2.888)	-0.074 (-0.117 to -0.017)	0.044 (-2.613)
MCC	-0.084 (-0.134 to -0.034)	0.027 (-3.269)	-0.017 (-0.073 to 0.028)	0.991 (-0.882)	-0.046 (-0.097 to 0.004)	0.500 (-1.802)	-0.078 (-0.129 to -0.028)	0.028 (-3.059)
Impulsivity								
SST region	Primary behaviour		Exploratory analyses					
	Impulsivity		Hyperactivity		Inattention		ODD/CD	
	R (95% CI)	<i>P</i> _{corrected} (t statistic)	R (95% CI)	<i>P</i> ^a (t statistic)	R (95% CI)	<i>P</i> ^a (t statistic)	R (95% CI)	<i>P</i> ^a (t statistic)
Left TPJ	-0.092 (-0.142 to -0.041)	0.009 (-3.570)	-0.067 (-0.117 to -0.016)	0.025 (-2.594)	-0.058 (-0.109 to -0.008)	0.062 (-2.270)	-0.071 (-0.118 to -0.017)	0.016 (-2.639)
Inattention								
SST region	Primary behaviour		Exploratory analyses					
	Inattention		Hyperactivity		Impulsivity		ODD/CD	
	R (95% CI)	<i>P</i> _{corrected} (t statistic)	R (95% CI)	<i>P</i> ^a (t statistic)	R (95% CI)	<i>P</i> ^a (t statistic)	R (95% CI)	<i>P</i> ^a (t statistic)
Right aIFS	-0.087 (-0.137 to -0.037)	0.019 (-3.392)	-0.017 (-0.068 to 0.033)	0.833 (-0.666)	-0.056 (-0.106 to -0.006)	0.073 (-2.184)	-0.084 (-0.126 to -0.026)	0.004 (-2.957)
ODD/CD behaviours								
SST region	Primary behaviour		Exploratory analyses					
	ODD/CD		Hyperactivity		Impulsivity		Inattention	
	R (95% CI)	<i>P</i> _{corrected} (t statistic)	R (95% CI)	<i>P</i> ^a (t statistic)	R (95% CI)	<i>P</i> ^a (t statistic)	R (95% CI)	<i>P</i> ^a (t statistic)
rlFC + anterior insula	-0.090 (-0.133 to -0.033)	0.011 (-3.246)	-0.014 (-0.065 to 0.036)	0.980 (-0.546)	-0.045 (-0.095 to 0.005)	0.295 (-1.754)	-0.053 (-0.109 to -0.003)	0.158 (-2.070)
Right aIFS	-0.084 (-0.126 to -0.026)	0.027 (-2.957)	-0.017 (-0.068 to 0.033)	0.954 (-0.666)	-0.056 (-0.106 to -0.006)	0.125 (-2.184)	-0.087 (-0.137 to -0.037)	0.005 (-3.392)

For each behaviour component, the prominent clusters in each brain network were identified if their univariate correlations with the sum of the corresponding behaviour items (that is, those in the column 'Primary behaviour') were significant after correction for multiple comparisons through 10,000 permutations (column '*P*_{corrected}'). For all prominent clusters identified in the first step, we further explored their univariate correlations with the remaining behaviour components (that is, those in the column 'Exploratory analyses'). See Supplementary Tables 2-4 for the complete results. *These *P* values were evaluated based on 10,000 permutations to correct for multiple comparisons in the corresponding exploratory tests.

P = 0.005; impulsivity: *R*² = 0.051; 90% CI = 0.033 to 0.069; adjusted *R*² = 0.024; *F*_(41, 1,464) = 1.92; *P* < 0.001; inattention: *R*² = 0.042; 90% CI = 0.026 to 0.059; adjusted *R*² = 0.016; *F*_(41, 1,464) = 1.58; *P* = 0.011),

the reward anticipation network showed a significant association with the total score of hyperactivity (*R*² = 0.043; 90% CI = 0.027 to 0.059; adjusted *R*² = 0.013; *F*_(46, 1,459) = 1.427; *P* = 0.033); however, we

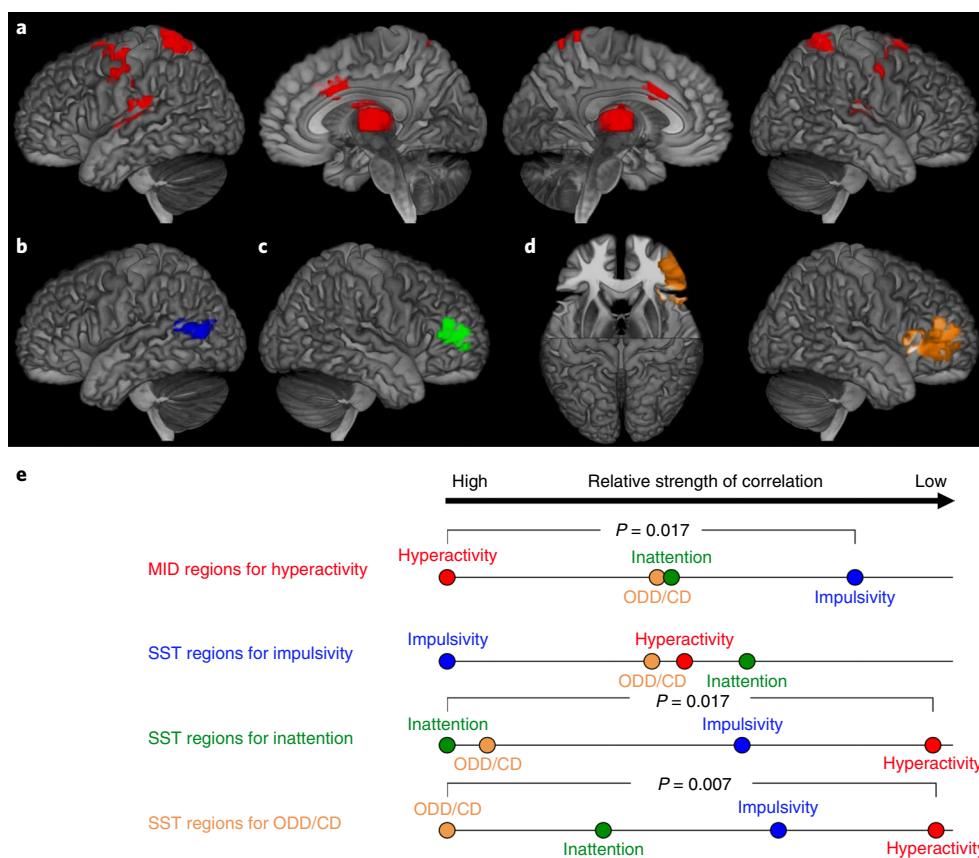


Fig. 3 | **a**, Reward anticipation network underlying hyperactivity (red; thalamus, SPL, mid-SC, PAC, MCC and SFJ). **b**, Motor inhibition network underlying impulsivity (blue; left middle TPJ). **c**, Motor inhibition network underlying inattention (green; right aIFS). **d**, Motor inhibition network underlying ODD/CD behaviours (orange; right inferior frontal gyrus + anterior insula and right aIFS). **e**, Neural signatures of ADHD and ODD/CD behaviours. For each neural network identified in **a–d**, its correlations with the corresponding primary behaviour and the rest of the ADHD or ODD/CD behaviours were compared and the corresponding relative strengths of the correlations are plotted (red: hyperactivity; blue: impulsivity; green: inattention; orange: ODD/CD behaviours). P values for pairwise significant differences after correction for multiple testing are provided.

found no evidence for an association with impulsivity ($R^2=0.027$; 90% CI=0.014 to 0.040; adjusted $R^2=-0.004$; $F_{(46, 1,459)}=0.885$; $P=0.691$) and inattention ($R^2=0.037$; 90% CI=0.022 to 0.052; adjusted $R^2=0.006$; $F_{(46, 1,459)}=1.214$; $P=0.156$).

fMRI signature for hyperactivity. The hyperactivity total score was significantly associated with reduced activation in six out of 46 brain regions in the reward anticipation network. These were the superior parietal lobule (SPL), middle central sulcus (mid-CS), thalamus, PAC, middle cingulate cortex (MCC) and superior frontal junction (SFJ) (Fig. 3a, Table 3 and Supplementary Table 2). We investigated the specificity of the observed associations and found that the SPL, mid-CS and thalamus were also associated with inattention. The mid-CS and MCC were associated with ODD/CD behaviours, whereas no significant association was found with impulsivity (Table 3 and Supplementary Table 2). The brain regions showed no significant difference in association strength with hyperactivity and with inattention ($\Delta Z_{\text{sum}}=-0.142$; 95% CI=-0.384 to 0.100; $P_{\text{perm}}=0.834$) or with ODD/CD behaviours ($\Delta Z_{\text{sum}}=-0.128$; 95% CI=-0.377 to 0.121; $P_{\text{perm}}=1$) (Table 4), and these associations were further found to be significantly smaller than a meaningful effect size with equivalence tests (inattention: $t=3.71$ and $P_{\text{one tailed}}<0.001$ for $\Delta Z_L=-0.10$; $t=6.02$; $P_{\text{one tailed}}<0.001$ for $\Delta Z_U=0.10$; ODD/CD behaviours: $t=3.71$ and $P_{\text{one tailed}}<0.001$ for $\Delta Z_L=-0.10$; $t=5.72$; $P_{\text{one tailed}}<0.001$ for $\Delta Z_U=0.10$). In contrast, the brain regions showed a significantly weaker association in the case of impulsivity ($\Delta Z_{\text{sum}}=-0.308$; 95% CI=-0.522 to -0.094; $P_{\text{perm}}=0.017$) (Table 4).

Thus, our findings suggest a shared specificity of brain activation during reward anticipation in hyperactivity, inattention and ODD/CD behaviours, but not in impulsivity (Fig. 3e).

However, in the motor inhibition network, despite the overall significant association, none of the six brain regions was significantly associated with hyperactivity (Supplementary Table 3a), suggesting that the observed overall association was based on multiple fMRI regions of the motor inhibition network, each with a minor contribution.

fMRI signature for impulsivity. The left temporoparietal junction (TPJ) of the motor inhibition network was associated with impulsivity ($R=-0.092$; 95% CI=-0.142 to -0.041; $t=-3.563$; $P_{\text{perm}}=0.010$) (Fig. 3b, Table 3 and Supplementary Table 3b), and additionally (in exploratory analyses) with hyperactivity ($R=-0.067$; 95% CI=-0.117 to -0.016; $t=-2.59$; $P_{\text{perm}}=0.025$) and ODD/CD behaviours ($R=-0.071$; 95% CI=-0.118 to -0.017; $t=-2.64$; $P_{\text{perm}}=0.016$), but not with inattention ($R=-0.058$; 95% CI=-0.109 to -0.008; $t=-2.270$; $P=0.062$) (Table 3 and Supplementary Table 3b), where no significant difference in the strength of association was observed ($\Delta Z_{\text{hyperactivity}}=-0.025$; 95% CI=-0.073 to 0.022; $P_{\text{perm}}=0.823$; $\Delta Z_{\text{inattention}}=-0.033$; 95% CI=-0.079 to 0.012; $P_{\text{perm}}=0.456$; $\Delta Z_{\text{ODD/CD}}=-0.021$; 95% CI=-0.069 to 0.027; $P_{\text{perm}}=1$) (Table 5). These associations were found to be significantly smaller than a meaningful effect size with equivalence tests (hyperactivity: $t=3.10$ and $P_{\text{one tailed}}<0.001$ for $L_{\Delta Z}=-0.10$; $t=5.17$ and $P_{\text{one tailed}}<0.001$ for $\Delta Z_U=0.10$; inattention: $t=2.86$ and $P_{\text{one tailed}}=0.002$

Table 4 | Evaluating the specificity of prominent brain regions for hyperactivity during reward anticipation

	$Z_{\text{hyperactivity}}$	$Z_{\text{impulsivity}}$	$Z_{\text{inattention}}$	$Z_{\text{ODD/CD}}$	Hyperactivity-impulsivity			Hyperactivity-inattention			Hyperactivity-ODD/CD						
					ΔZ (95% CI)	Steiger's Z statistic	P_{Steiger}	P_{perm}	ΔZ (95% CI)	Steiger's Z statistic	P_{Steiger}	P_{perm}	ΔZ (95% CI)	Steiger's Z statistic	P_{Steiger}	P_{perm}	
Thalamus	-0.091	-0.039	-0.075	-0.065	-0.052 (-0.100 to -0.005)	-2.270	0.023	0.024	0.024	-0.016 (-0.070 to 0.036)	-0.634	0.526	0.526	-0.026 (-0.080 to 0.029)	-0.955	0.340	0.342
SFJ	-0.084	-0.023	-0.067	-0.053	-0.061 (-0.111 to -0.011)	-2.670	0.008	0.008	0.008	-0.017 (-0.070 to 0.035)	-0.686	0.493	0.491	-0.031 (-0.090 to 0.028)	-1.156	0.248	0.247
PAC	-0.085	-0.037	-0.048	-0.064	-0.048 (-0.089 to -0.007)	-2.091	0.037	0.036	0.036	-0.037 (-0.086 to 0.012)	-1.472	0.141	0.139	-0.021 (-0.071 to 0.028)	-0.787	0.431	0.431
SPL	-0.094	-0.053	-0.077	-0.068	-0.041 (-0.088 to 0.002)	-1.801	0.072	0.070	0.070	-0.017 (-0.065 to 0.031)	-0.681	0.496	0.496	-0.026 (-0.080 to 0.028)	-0.976	0.329	0.328
Mid-CS	-0.092	-0.048	-0.074	-0.075	-0.044 (-0.107 to 0.001)	-1.893	0.058	0.058	0.058	-0.017 (-0.066 to 0.031)	-0.678	0.498	0.496	-0.017 (-0.072 to 0.038)	-0.627	0.531	0.529
MCC	-0.084	-0.023	-0.046	-0.078	-0.062 (-0.107 to -0.016)	-2.676	0.008	0.008	0.008	-0.038 (-0.088 to 0.013)	-1.503	0.133	0.133	-0.006 (-0.057 to 0.045)	-0.225	0.822	0.822
Sum	-0.530	-0.222	-0.388	-0.402	-0.308 (-0.522 to -0.094)		0.006	0.006	0.006	-0.142 (-0.384 to 0.100)		0.278	0.278	-0.128 (-0.377 to 0.121)		0.411	0.411

The specificity of prominent brain regions for hyperactivity was evaluated by comparing their correlations and associations with those for the rest of the behaviours (that is, the ADHD constructs impulsivity and inattention, as well as ODD/CD behaviours). For each brain region, its correlations with all behaviours were first transformed into normally distributed Z scores (columns labelled ' $Z_{\text{hyperactivity}}$ ', ' $Z_{\text{impulsivity}}$ ', ' $Z_{\text{inattention}}$ ', and ' $Z_{\text{ODD/CD}}$ ') through the Fisher transformation, and the pairwise differences (columns labelled ' ΔZ ') were then tested against the null using both Steiger's test (columns labelled 'Steiger's Z statistic' and ' P_{Steiger} ') and permutation test (column labelled ' P_{perm} '), both of which provided very similar results. The overall significance throughout all brain regions was then evaluated based on the summed ΔZ value across all brain regions using a permutation test. The number of permutations was set to 10,000. All P values presented in the table were based on two-tailed tests without correction for multiple testing.

Table 5 | Evaluating the specificity of prominent brain regions for impulsivity, inattention and ODD/CD during motor inhibition

	Impulsivity			Inattention			ODD/CD			Impulsivity-hyperactivity			Impulsivity-inattention			Impulsivity-ODD/CD		
	Z _{impulsivity}	Z _{hyperactivity}	Z _{inattention}	Z _{impulsivity}	Z _{inattention}	Z _{ODD/CD}	ΔZ (95% CI)	Steiger's Z statistic	P _{Steiger}	P _{perm}	ΔZ (95% CI)	Steiger's Z statistic	P _{Steiger}	P _{perm}	ΔZ (95% CI)	Steiger's Z statistic	P _{Steiger}	P _{perm}
Left TPJ	-0.092	-0.067	-0.059	-0.071	-0.025 (-0.073 to 0.022)	-1.090 (-0.073 to 0.022)	-0.025 (-0.073 to 0.022)	-1.090	0.276	0.274	-0.033 (-0.079 to 0.012)	-1.429	0.153	0.152	-0.021 (-0.069 to 0.027)	-0.886	0.375	0.375
Inattention																		
	Z _{inattention}	Z _{hyperactivity}	Z _{impulsivity}	Z _{ODD/CD}	Inattention-hyperactivity			Inattention-impulsivity			Inattention-ODD/CD							
					ΔZ (95% CI)	Steiger's Z statistic	P _{Steiger}	P _{perm}	ΔZ (95% CI)	Steiger's Z statistic	P _{Steiger}	P _{perm}	ΔZ (95% CI)	Steiger's Z statistic	P _{Steiger}	P _{perm}		
Right aIFS	-0.087	-0.017	-0.056	-0.084	-0.070 (-0.124 to -0.017)	-2.795	0.005	0.006	-0.031 (-0.080 to 0.018)	-1.330	0.184	0.187	-0.004 (-0.052 to 0.045)	-0.146	0.884	0.884		
ODD/CD																		
	Z _{ODD/CD}	Z _{hyperactivity}	Z _{impulsivity}	Z _{inattention}	ODD/CD-hyperactivity			ODD/CD-impulsivity			ODD/CD-inattention							
					ΔZ (95% CI)	Steiger's Z statistic	P _{Steiger}	P _{perm}	ΔZ (95% CI)	Steiger's Z statistic	P _{Steiger}	P _{perm}	ΔZ (95% CI)	Steiger's Z statistic	P _{Steiger}	P _{perm}		
rIFC + anterior insula	-0.090	-0.014	-0.045	-0.053	-0.076 (-0.128 to -0.024)	-2.821	0.005	0.004	-0.045 (-0.096 to 0.005)	-1.896	0.058	0.058	-0.037 (-0.086 to 0.012)	-1.530	0.129	0.131		
Right aIFS	-0.084	-0.017	-0.056	-0.087	-0.067 (-0.118 to -0.015)	-2.465	0.013	0.013	-0.028 (-0.077 to 0.022)	-1.156	0.248	0.251	0.004 (-0.045 to 0.052)	0.146	0.884	0.884		
Sum	-0.174	-0.031	-0.102	-0.141	-0.143 (-0.237 to -0.049)		0.002	0.002	-0.073 (-0.164 to 0.019)		0.091	0.091	0.041 (-0.122 to 0.055)		0.390	0.390		

The specificity of prominent brain regions for the corresponding behaviours was evaluated by comparing their correlations/associations with those with the rest behaviours from ADHD constructs and ODD/CD behaviours. For each brain region, its correlations with all behaviours were first transformed into normally distributed Z-scores (columns labelled 'Z_{hyperactivity}', 'Z_{impulsivity}', 'Z_{inattention}' and 'Z_{ODD/CD}', respectively) through the Fisher transformation, and the pairwise differences (column labelled 'ΔZ') were then tested using both Steiger's test (Columns labelled 'Steiger's Z statistic' and 'P_{Steiger}') and the permutation test (column labelled 'P_{perm}'), both of which provided very similar results. When there were multiple prominent regions, their overall significance was then evaluated based on the summed absolute ΔZ across all brain regions using a permutation test. The number of permutations was set to 10,000. All P-values were based on two-tailed tests without correction for multiple testing.

for $L_{\Delta Z} = -0.10$; $t = 5.73$ and $P_{\text{one tailed}} < 0.001$ for $\Delta Z_U = 0.10$; ODD/CD behaviours: $t = 3.21$ and $P_{\text{one tailed}} < 0.001$ for $L_{\Delta Z} = -0.10$; $t = 4.93$ and $P_{\text{one tailed}} < 0.001$ for $\Delta Z_U = 0.10$). Together, this suggests a shared specificity across ADHD and ODD/CD behaviours during motor inhibition (Fig. 3e).

fMRI signature for inattention. In the motor inhibition network, we found significant association of the right anterior inferior frontal sulcus (aIFS) with inattention ($R = -0.087$; 95% CI = -0.137 to -0.037 ; $t = -3.392$; $P_{\text{perm}} = 0.019$), as well as (in exploratory analyses) association with ODD/CD behaviours ($R = -0.084$; 95% CI = -0.126 to -0.026 ; $t = -2.957$; $P_{\text{perm}} = 0.004$), but not with impulsivity ($R = -0.056$; 95% CI = -0.106 to -0.006 ; $t = -2.184$; $P_{\text{perm}} = 0.073$) and hyperactivity ($R = -0.017$; 95% CI = -0.068 to 0.033 ; $t = -0.666$; $P_{\text{perm}} = 0.833$) (Fig. 3c, Table 3 and Supplementary Table 3c). The strength of association of aIFS with inattention was not significantly different from those with impulsivity ($\Delta Z = -0.031$; 95% CI = -0.080 to 0.018 ; $P_{\text{perm}} = 0.562$) and ODD/CD behaviours ($\Delta Z = -0.004$; 95% CI = -0.052 to 0.045 ; $P_{\text{perm}} = 1$) (Table 5), and these associations were further found to be significantly smaller than a meaningful effect size with equivalence tests (impulsivity: $t = 2.77$ and $P_{\text{one tailed}} = 0.003$ for $L_{\Delta Z} = -0.10$; $t = 5.26$ and $P_{\text{one tailed}} < 0.001$ for $\Delta Z_U = 0.10$; ODD/CD: $t = 3.98$ and $P_{\text{one tailed}} < 0.001$ for $L_{\Delta Z} = -0.10$; $t = 4.18$ and $P_{\text{one tailed}} < 0.001$ for $\Delta Z_U = 0.10$). However, the strength of association of aIFS with inattention was significantly stronger than that with hyperactivity ($\Delta Z = -0.070$; 95% CI = -0.124 to -0.017 ; $P_{\text{perm}} = 0.017$) (Table 5), suggesting distinct specificities of hyperactivity and inattention during motor inhibition, and shared specificity of inattention with impulsivity and ODD/CD behaviours (Fig. 3e).

fMRI signatures for ODD/CD behaviours. ODD/CD behaviours were found only in a significant canonical correlation with the motor inhibition network. The right aIFS ($R = -0.084$; 95% CI = -0.126 to -0.026 ; $t = -2.96$; $P_{\text{perm}} = 0.027$) and rIFC/anterior insula ($R = -0.090$; 95% CI = -0.133 to -0.033 ; $t = -3.25$; $P_{\text{perm}} = 0.011$) were associated with the summed score of ODD/CD behaviours (Fig. 3d, Table 3 and Supplementary Table 4). While both regions were also significantly associated with ODD behaviours alone, and the rIFC/anterior insula was associated with CD behaviours (Supplementary Table 4), their association strength with ODD behaviours was significantly stronger than that with CD behaviours ($\Delta Z_{\text{sum}} = -0.090$; 95% CI = -0.175 to -0.006 ; $P_{\text{perm}} = 0.039$), suggesting a predominant role of ODD behaviours in the associations with both brain regions. Together, prominent ODD/CD regions showed no significant difference in association strength with ODD/CD behaviours and with inattention ($\Delta Z_{\text{sum}} = -0.041$; 95% CI = -0.122 to 0.055 ; $P_{\text{perm}} = 1$), nor with impulsivity ($\Delta Z_{\text{sum}} = -0.073$; 95% CI = -0.164 to 0.019 ; $P_{\text{perm}} = 0.274$) (Table 5), and these associations were found to be significantly smaller than a meaningful effect size with equivalence tests (inattention: $t = 3.68$ and $P_{\text{one tailed}} < 0.001$ for $L_{\Delta Z} = -0.10$; $t = 5.16$ and $P_{\text{one tailed}} < 0.001$ for $\Delta Z_U = 0.10$; impulsivity: $t = 2.72$ and $P_{\text{one tailed}} = 0.003$ for $L_{\Delta Z} = -0.10$; $t = 5.83$ and $P_{\text{one tailed}} < 0.001$ for $\Delta Z_U = 0.10$), but significantly lower than the association strength with hyperactivity ($\Delta Z_{\text{sum}} = -0.0143$; 95% CI = -0.237 to -0.049 ; $P_{\text{perm}} = 0.007$) (Fig. 3e and Table 5).

In conclusion, ADHD and ODD/CD may share several distinctive neural bases during reward anticipation and motor inhibition.

Discussion

Here, we characterize clinically relevant behaviours in adolescents by describing brain activation during reinforcement-related cognitive processes. These behaviours include externalizing symptoms of hyperactivity, impulsiveness, inattention, oppositional defiance and conduct, and internalizing symptoms of anxiety and depression. We have used quantitative measures to assess these behaviours, as

empirical evidence shows that psychopathology is generally more dimensional than categorical²⁸—one of the basic premises of the research domain criteria²⁹. We interrogated the neural basis of each of these behaviours by measuring brain activity during reinforcement-related cognitive tasks of reward processing, motor inhibition and social-emotional processing.

We found that activation of similar brain regions is often associated with different tasks (and behaviours). While well-known representative brain areas (for example, the ventral striatum and OFC for reward anticipation⁸, the rIFC for inhibitory control⁹, and the amygdala and STS for social-emotional processing^{10,11}) were activated as expected, these activations were not restricted to one task alone (Fig. 2d). This might represent the involvement of shared cognitive components in different behaviours that might be less specific to individual tasks. For example, the ventral striatum activation during motor inhibition was due to the anticipation of a random event³⁰, thus the anticipatory component was shared with the reward anticipation network, which activates the same region. In some instances, it may also be caused by brain activation that reflects task presentation (for example, motor cortex activation in the active MID task and SST, but not during passive viewing in the EFT). Our observation is consistent with the notion of a basic neural function that underlies a complex profile of different behaviours³¹.

However, the overlap of brain activation across cognitive tasks might also indicate the presence of different functional or structural domains within a given brain region that relate differentially to each task³². This latter hypothesis is supported by the observation of low correlations of the same brain regions across tasks. In contrast, we found high correlations between different brain regions within each task, suggesting network constellations that are specific to each individual cognitive task. This specificity was further suggested by the observation that the variances of hyperactivity explained by reward anticipation and motor inhibition networks are additive (that is, the adjusted R^2 values were 0.033, 0.013 and 0.018 for both networks, reward anticipation and motor inhibition, respectively), and thus not overlapping. The specificity of cognitive neural networks might thus be defined as much by their internal collaborative structure as by the individual brain regions involved³³.

We also found highly activated regions (Cohen's $D > 0.30$) in the MID task that were not expected to be activated in the anticipation of a visually presented reward. These included the PAC, which we observed to be activated in the absence of any auditory stimulus. As the PAC has been found to predict reward value¹⁶ and is associated with anticipatory motor response³⁴ upon auditory stimulation, our findings point towards the possibility of the PAC underlying these cognitive processes in a way that is not dependent on the quality of the sensory stimulus. In addition, wide areas within the somatosensory cortex were also activated in the MID task, further suggesting the recruitment of sensory cortices (including the visual cortices) during reward anticipation irrespective of the quality of the signal input³⁵.

We found a strong overall correlation (adjusted $\eta^2 = 0.160$; that is, 16% of variance was explained after adjusting for inflation due to the involvement of multiple variables) of neural networks with externalizing behaviours (ADHD and ODD/CD), particularly in reward anticipation and motor inhibition, but did not observe a significant correlation with internalizing behaviours (adjusted $\eta^2 = -0.024$). While ADHD behaviours were related to both reward anticipation and motor inhibition networks, we found specific neural signatures that distinguished each of the individual behaviours. While brain activity in the reward anticipation network was correlated with both hyperactivity and inattention (Table 3), their activation patterns were not significantly different (Fig. 3e and Table 4), and were in fact equivalent. However, in the motor inhibition network, the correlation with inattention was significantly stronger than that with hyperactivity (Fig. 3e and Tables 3 and 5), consistent

with a greater effort to maintain sustained attention during the task. This interpretation is supported by the strong correlation during successful motor inhibition of inattention with rIFC activity (Fig. 3c and Table 3)—a brain region previously implicated in attentional detection, monitoring and motor inhibition⁹.

In contrast, for impulsivity, we found no significant correlation with the reward anticipation network. In the motor inhibition network, its strongest correlation was with activation of the left TPJ (Fig. 3b and Table 3), which, however, shows no significant differences from (and in practice, appears equivalent to) the correlations between left TPJ activation and both hyperactivity and inattention (Fig. 3e and Table 5). This observation is in line with the previous finding of reduced bilateral TPJ activity in patients with ADHD³⁶.

We thus identified neural signatures that distinguish hyperactivity, inattention and impulsivity on the basis of brain activation patterns during reward anticipation and motor inhibition. These signatures enable a more refined characterization of ADHD behaviour than the currently used distinction between motivational and motor inhibitory processes³⁷.

ODD/CD behaviours were related to the motor inhibition network, but not reward anticipation, which is in line with previous findings^{38,39}. Activation patterns for ODD and CD behaviours in the motor inhibition network were similar, although dominated by ODD behaviours, suggesting a shared neural basis (Supplementary Table 4)⁴⁰. Surprisingly, we were not able to distinguish between activation patterns in the motor inhibition network in conduct and inattention symptoms (Fig. 3c–e and Tables 3 and 5), which were also found to be practically equivalent. While this may indicate in part a shared neural basis, the phenotypic differences between these behaviours also suggest the presence of a distinguishing cognitive domain, which we did not capture in our tasks. Nevertheless, the shared neural signatures between ODD/CD and ADHD symptoms indicate a shared neural basis underlying the high comorbidity between ODD/CD and ADHD^{41,42}, supporting the idea of unifying ADHD and ODD/CD into a single spectrum disorder⁴³.

It is a limitation of this work (and indeed of all task-based fMRI studies) that none of the tasks selected represents all aspects of the behavioural domain interrogated. For example, the research domain criteria divide reward processing into three different constructs and nine sub-constructs. The MID task interrogates only two sub-constructs: reward anticipation and early response to reward. Nonetheless, it is well established that the MID task, SST and EFT capture important and clinically relevant aspects of reward processing¹², impulsiveness (in particular, response inhibition)⁴⁴ and social-emotional processing¹⁰, respectively. While we showed distinctive patterns in neural networks that stratify ADHD subtypes/components during reward anticipation (that is, the motivational pathway) and motor inhibition, the explained variance from individual regions of these neural networks is low ($R^2 < 1\%$), which might be partly due to a task-dependent, incomplete representation of neural pathways underlying ADHD. However, given that together the neural networks could explain up to 16% of the variance of externalizing behaviours (that is, adjusted $\eta^2 = 0.160$ for RCCA after adjusting for the number of variables; also note that this effect could be even larger should the ridge regularization not be applied), the observed small effect size in the univariate analyses might be due to two additional factors. First, the current behavioural constructs (for example, hyperactivity, impulsivity and inattention of ADHD) might themselves hide heterogeneity, leading to reduced explanation of variance. Second, neural networks might not be homogenous (for example, despite a significant overall association of the motor inhibition network with hyperactivity across all 40 brain clusters (adjusted $R^2 = 0.018$), no cluster survived correction for multiple comparisons; Supplementary Table 3a). This is in striking contrast with the greater homogeneity of the reward anticipation network, for which six out of 46 brain clusters were in significant association

with hyperactivity (Table 3 and Supplementary Table 2), despite smaller overall explained variance (adjusted $R^2 = 0.013$). Thus, the reduced effect size may highlight the heterogeneity of behavioural components as well as neural networks.

Our approach provides a unified framework with which to investigate brain activity in reinforcement-related behaviour, enabling the characterization of shared and distinct functional brain activation patterns that underlie different externalizing symptoms. It also resulted in the identification of neural signatures that may help to stratify these symptoms, while accounting for clinically observed comorbidity.

Methods

Ethical approval. The IMAGEN study was approved by local research ethics committees at each research site (King's College London, the University of Nottingham, Trinity College Dublin, the University of Heidelberg, Technische Universität Dresden, Commissariat à l'Énergie Atomique et aux Énergies Alternatives and the University Medical Center. Informed consent was sought from all participants and a parent or guardian of each participant.

Participants. Complete data on fMRI and behavioural measurements for 1,506 adolescents (mean age = 14.44 years; s.d. = 0.42 years; range = 12.88–16.44 years; female-to-male ratio = 783/723) from the baseline assessment of the IMAGEN sample were included in the analyses. Of the 1,506 participants investigated in this study, clinical DAWBA ratings were available from 1,190 individuals. Of these individuals, 131 had one or more diagnoses: 33 individuals were diagnosed with ADHD, 59 had emotional problems, 12 had anxiety (general + other) and 33 had depression (major + other). Detailed descriptions of this study have previously been published⁴. Gender, handedness and imaging sites were regressed out before the canonical correlation analyses were conducted, and for the rest of the analyses.

SDQ and DAWBA. The SDQ⁴⁵ is a brief 25-item behavioural screening tool probing hyperactivity, emotional symptoms, conduct problems, peer problems and prosocial behaviour in 3- to 16-year-old children. In the current study, we chose parent-rated hyperactivity (five items) and conduct problems (five items) to represent externalizing problems, and child-rated emotional problems (five items) to represent internalizing problems (Table 1). This choice was based on findings that externalizing problems scores from parents are more reliable than those from children themselves, and vice versa⁴⁶.

In DAWBA⁴⁷, similar to SDQ, parent-rated ADHD and ODD/CD items, as well as child-rated specific phobia, social phobia, general anxiety, fear and depression items (Table 1), were included in the analyses.

fMRI data acquisition and analysis. Structural and functional MRI data were acquired at eight IMAGEN assessment sites with 3T MRI scanners from different manufacturers (Siemens, Philips, General Electric and Bruker). The scanning variables were specifically chosen to be compatible with all scanners. The same scanning protocol was used at all sites. In brief, high-resolution T1-weighted three-dimensional structural images were acquired for anatomical localization and co-registration with the functional time series. BOLD functional images were acquired with a gradient-echo, echo-planar imaging sequence. For all tasks, 300 volumes were acquired for each participant, and each volume consisted of 40 slices aligned to the anterior commissure/posterior commissure line (2.4-mm slice thickness; 1 mm gap). The echo time was optimized (echo time = 30 ms; repetition time = 2,200 ms) to provide reliable imaging of subcortical areas.

Functional MRI data were analysed with SPM8 (<http://www.fil.ion.ucl.ac.uk/spm>). Spatial pre-processing included: slice time correction to adjust for time differences due to multi-slice imaging acquisition; realignment to the first volume in line; nonlinear warping to the MNI (Montreal Neurological Institute) space (based on a custom echo-planar imaging template (53 × 63 × 46 voxels) created out of an average of the mean images of 400 adolescents); resampling at a resolution of 3 × 3 × 3 mm³; and smoothing with an isotropic Gaussian kernel a full width at half-maximum value of 5 mm.

At the first level of analysis, changes in the BOLD response for each subject were assessed by linear combinations of experimental conditions at the individual subject level. For each experimental condition (for example, the large win condition during the anticipation phase of the MID task), each trial was convolved with the haemodynamic response function to form regressors that accounted for potential noise variance (for example, head movement) associated with the processing of reward anticipation. Estimated movement parameters were added to the design matrix in the form of 18 additional columns (three translations, three rotations, three quadratic translations and three cubic translations, plus a shift of ± 1 TR (repetition time) for each translation).

For the MID task anticipation phase, we contrasted brain activation during anticipation of a large win (represented by a circle with three horizontal lines in Fig. 1 and Extended Data Fig. 5) versus anticipation of no win (represented by

a triangle in Fig. 1 and Extended Data Fig. 5). For the EFT, we contrasted brain activation during viewing of an angry face versus a viewing control (circles). For the SST, we contrasted brain activation during successful stop versus successful go. The single-subject contrast images were then used in the population-based weighted voxel co-activation network analysis.

MID task for fMRI. Participants performed a modified version of the MID task to examine neural responses to reward anticipation and reward outcome²⁰. The task consisted of 66 10-s trials. In each trial, participants were presented with one of three cue shapes (250 ms) denoting whether a target (white square) would subsequently appear on the left or right side of the screen and whether zero, two or ten points could be won in that trial. After a variable delay (4,000–4,500 ms) of fixation on a white crosshair, participants were instructed to respond with a left or right button press as soon as the target appeared. Feedback on whether and how many points were won during the trial was presented for 1,450 ms after the response (Extended Data Fig. 5)⁶. Using a tracking algorithm, task difficulty (that is, target duration, which varied between 100 and 300 ms) was individually adjusted such that each participant successfully responded on ~66% of trials. Participants had first completed a practice session outside the scanner (~5 min), during which they were instructed that for each five points won they would receive one food snack in the form of small chocolate candies.

Based on previous research suggesting reliable associations between ADHD symptoms and fMRI BOLD responses measured during reward anticipation, the current study used the contrast of anticipation of a high win versus anticipation of no win. Only successfully hit trials were included here.

Emotional reactivity fMRI model (EFT). This task was adapted from ref. ²². Participants watched 18-s blocks of either a face video (depicting anger or neutrality) or a control stimulus (Extended Data Fig. 6)²². Each face video comprised a black and white video clip (200–500 ms) of a male or female face. Five blocks each of angry and neutral expressions were interleaved with nine blocks of the control stimulus. Each block contained eight trials of six face identities (three female). The same identities were used for the angry and neutral blocks. The control stimuli were black and white concentric circles expanding and contracting at various speeds that roughly matched the contrast and motion characteristics of the face clips.

The neutral blocks contained emotional expressions that were not attributable to any particular emotion (for example, nose twitching); however previous research has suggested that neutral stimuli are not always interpreted as such. Functional imaging studies have found significant activation of the amygdala in response to the presentation of neutral faces in healthy adult males⁴⁸, patients with social anxiety and matched control participants⁴⁹, adolescents with conduct disorder problems⁵⁰ and young men with violent behaviour problems⁵¹. This suggests that neutral faces may be interpreted as emotionally ambiguous. This study focused specifically on the effects of viewing angry faces (versus control faces) to eliminate this ambiguity so that any significant relationships between behaviour and brain activity could be interpreted as the consequence of viewing negative social stimuli (anger).

SST for fMRI. Participants performed an event-related SST designed to study neural responses to successful and unsuccessful inhibitory control²¹. The task was composed of go trials and stop trials. During go trials (83%; 480 trials), participants were presented with arrows pointing either to the left or to the right. During these trials, subjects were instructed to make a button response with their left or right index finger corresponding to the direction of the arrow. In the unpredictable stop trials (17%; 80 trials), the arrows pointing left or right were followed (on average, 300 ms later) by arrows pointing upwards; participants were instructed to inhibit their motor responses during these trials (Extended Data Fig. 7)⁵². A tracking algorithm changed the time interval between go signal and stop signal onsets according to each subject's performance on previous trials (average percentage of inhibition over previous stop trials, recalculated after each stop trial), resulting in 50% successful and 50% unsuccessful inhibition trials. The inter-trial interval was 1,800 ms. The tracking algorithm of the task ensured that subjects were successful on 50% of stop trials and worked at the edge of their own inhibitory capacity.

Population-based WVCNA. The WVCNA^{12,18} was applied to parcellate those highly co-activated voxels in all three fMRI contrasts (for example, the large win versus no win contrast anticipation phase of the MID task, the angry face versus control contrast of the EFT, and the successful stop versus successful go contrast of the SST). Such a parcellation procedure could effectively reduce the dimensionality without losing too much information. The procedure is summarized below.

Pre-processing. For all three tasks, the initial pre-processing steps involved removing null voxels (including out-brain voxels based on an automated anatomical labelling template) and potential participant outliers from the contrast data based on low inter-sample correlations. The activation maps of pre-processed data were then generated, and only those positive activations with at least a medium effect size (that is, Cohen's $D > 0.3$; see the following section for more details) were included in the following analyses.

Parameter selection. To minimize the arbitrary choice of parameters, we took the default and suggested settings of the R package WGCNA⁵³, except for the soft thresholds of adjacency matrices, which were determined as seven for the MID task, eight for the EFT and seven for the SST, based on the fitness of scale-free topology criteria (Extended Data Fig. 8). The above adjacency matrices were then used to generate the topology overlapping matrices, which captured both the direct and indirect connections among voxels. The hierarchical clustering was then applied on the distance matrices as 1 minus the topology overlapping matrices and, together with the dynamic cut-tree function, the fMRI modules were generated as functional ROIs. The first principle component of each module was included in the following analysis to represent brain activation (or BOLD response). No merge of modules was conducted after the hierarchical clustering to avoid using an arbitrary threshold.

Effect size threshold for brain activation. Cohen's D was defined as $\frac{\beta_1 - \beta_2}{\sigma_{\text{pooled}}}$. Cohen proposed (reluctantly) to use Cohen's $D = 0.5$ for a two-sample t -test, as well as an alternative option of using the correlation coefficient $r = 0.3$ as the threshold for a median effect size²⁷. As pointed out by Cohen, these two effect sizes (that is, D and r) could be mutually transformed (that is, a two-sample t -test could alternatively be understood as testing for a correlation between the group label and the pooled sample) so that (in case the variances are equal in both groups and the total sample is N):

$$\frac{t}{\sqrt{N}} = \frac{D_{2\text{-sample}}}{k} = \frac{r}{\sqrt{1-r^2}}$$

where t is the t statistic and k is determined by the percentage of each group in the full sample (that is, p and q , respectively) as $\sqrt{1/pq}$, for which the minimum value 2 is acquired when the sample sizes are equal in both groups (that is, $p = q$). A clear difference between D and r in a two-sample t -test could therefore be readily understood as while the achieved statistical power depends on the exact sample size in each group for Cohen's D , the achieved statistical power of r (that is, the correlation coefficient) only depends on the full sample size. Therefore, the proposed thresholds for median effect size (that is, $D = 0.5$ and $r = 0.3$) are not equivalent, and $r = 0.3$ is more stringent than $D = 0.5$ ($r \leq 0.243$ depending on the exact sample size in each group). This highlights the fact that the choice of a threshold for effect size is flexible in certain ways, if not completely arbitrary.

However, in the case of a one-sample t -test with the same definition of D , the relationship between the t statistic and effect size D now changes to $\frac{t}{\sqrt{N}} = D_{1\text{-sample}}$.

Therefore, Cohen's D in a one-sample t -test shares a similar relationship to the achieved statistical power with the correlation coefficient r in a two-sample t -test in that only the total sample size matters. Therefore, to achieve the same statistical power as for $r = 0.30$ (that is, the threshold of the median effect size) with the same sample size, the equivalent Cohen's D of a one-sample t -test could be calculated as 0.32.

In addition, Cohen²⁷ also discussed the differences in Cohen's D between two-sample and one-sample t -tests (case 3 in chapter 2). He suggested using the transformation $D_{1\text{-sample}} = D_{2\text{-sample}}/\sqrt{2}$ to re-calculate the critical values for the one-sample t -test, for which the corresponding threshold of the median effect size is therefore $D = 0.35$. However, this transformation aims to achieve equal statistical power between the one-sample and two-sample t -tests on the condition that the sample size in the one-sample t -test is half of that in the two-sample t -test, with balanced sample sizes in both groups.

Despite alternative strategies in calculation, both thresholds are indeed similar; therefore, we used Cohen's $D = 0.30$ as the threshold of the median effect size for a one-sample t -test, which is agreeable with both calculations when keeping one decimal.

RCCA. Canonical correlation analyses (CCAs) have been widely used to investigate the overall correlation between two sets of variables⁵⁴. However, in our case, due to high intra-correlations in both brain fMRI networks and behavioural items, multicollinearity was a potential risk factor that could jeopardize the validity of following statistical inference. Therefore, we adopted the RCCA proposed by ref. ¹⁹, where two ridge-regularization parameters, λ_x and λ_y , are added to the diagonals of corresponding covariance matrices to avoid the singularity.

As our purposes were not to maximize the power of prediction, instead of estimating the optimal regulation parameters⁵⁵, we fixed the regulation parameters across all analyses. Although multiple predefined regulation parameters were investigated (that is, 0.1, 0.2, 0.3, 0.4 and 0.5) for both λ values, the significance of major results was consistent throughout all settings (Extended Data Fig. 3); therefore, we simply report the P values and relevant statistics based on the regulation parameter 0.1. It is also noteworthy that optimization of the regulation parameter almost surely invalidates any attempt to calculate internalized P values through the permutation test, unless the optimization procedure is also permuted, which is very difficult (if not impossible) due to the extremely high computational demands of optimization at each iteration. It should also be noted that current optimization procedures of CCA-related approaches focus on maximizing the prediction power for the first component and are therefore not a real optimum for our purpose of evaluating the overall correlation described below.

RCCA was then applied on two sets of standardized variables to investigate their overall correlation. For each correlation, the P value or significance level was determined using permutation tests, where the individual IDs of behaviour items were randomly shuffled at each iteration to generate the null distribution of statistics of interest. Particularly, we used the eta square (η^2) to represent the proportion of mutually explained variance between the two sets of variables. This is analogous to the R^2 value (that is, the coefficient of determination) in a multiple linear model. η^2 was defined as $1 - \lambda_{\text{Wilks}}$, where λ_{Wilks} (Wilks's lambda) is a commonly used effect size in CCA⁵⁶ and could be calculated as the multiplication of unexplained variance for the correlation of each pair of components:

$$\lambda_{\text{Wilks}} = \prod_{i=1}^k (1 - \rho_i^2)$$

where ρ_i^2 denotes the squared correlation (that is, the mutually explained variance) between the i th pair of RCCA components, and k denotes the total number of CCA components for each set of variables. Note that η^2 , similar to R^2 , increased when more variables were included in the CCA, even if all of these variables were completely irrelevant. Therefore, we further included an adjusted η^2 (analogous to the adjusted R^2) to correct for the inflation in η^2 caused by the increased number of variables as:

$$\eta_{\text{adj}}^2 = 1 - \frac{1 - \eta^2}{1 - \eta_0^2}$$

where η_0^2 represents the expected η^2 under the null hypothesis that there is no relationship between the two sets of variables (that is, it acts as a measure of inflation in η^2), and can be directly estimated through the permutation test. Clearly, η_{adj}^2 is a monotonic increasing function of η^2 , where η_{adj}^2 tends to 0 when $\eta^2 \rightarrow \eta_0^2$, and to 1 when $\eta^2 \rightarrow 1$.

The standard error (s.e.) of η^2 was then estimated using Jackknife^{57,58}, and the corresponding 90% confidence intervals were calculated as $[Z_{5\%} \times \text{s.e.}_{\eta^2} + \eta^2, Z_{95\%} \times \text{s.e.}_{\eta^2} + \eta^2]$, where $Z_{x\%}$ denotes the Z score at the $x\%$ quantile of a standardized normal distribution.

Comparison of related associations/correlations through permutation. To compare two correlations, a Fisher's transformation is normally applied to first normalize the distributions of correlations. The transformed correlations, now following the normal distribution, can then be compared directly, and the corresponding differences should also follow a normal distribution⁵⁹. However, estimation of the variance of such a difference should properly consider the relationship of variables involved in calculating the correlations. For example, in the present paper, we are interested in the difference between two correlations that share one variable in common (that is, in the form of $\text{cor}(A,B)$ versus $\text{cor}(A,C)$). While the analytical solution of the variance estimation for the above case has been extensively investigated in the past^{60–62}, we additionally implemented the permutation process to empirically investigate the variance, which is not only known to be robust even if the normality assumption has been violated, but also enables us to investigate multiple comparisons together, where the variance of summed absolute differences under the null hypothesis could be directly estimated through the permutation process.

In the present paper, we directly calculated the P value (which was determined by the underlying variance) of the observed summed absolute difference through a permutation process as the chance of randomly observing (that is, at each permutation iteration) a summed absolute difference larger than the original observation. For comparison purposes, we included the results from Steiger's test⁶¹ in the relevant tables, which were highly similar to the results using the permutation test.

Equivalence test. Whenever a null result was observed from a statistical test, no meaningful statistical inference could be drawn unless a proper test was conducted to show that the observed non-significant effect size was indeed smaller than a meaningful threshold. In the present study, we adopted the equivalence test through a 'two one-sided test' procedure²⁶ in which the observed effect size was tested against a lower equivalence bound (with a null hypothesis that the observed effect size was lower than this lower bound) and an upper equivalence bound (with a null hypothesis that the observed effect size was larger than this upper bound). If both tests were significant, we could then conclude that the observed effect size was statistically smaller than a meaningful one; hence, in a sense, equivalent to zero. In cases in which we were only interested in a one-tailed test (for example, we were only interested in a positive correlation or R^2), it was "also possible to test for inferiority, or the hypothesis that the effect is smaller than an upper equivalence bound, by setting the lower equivalence bound to ∞ "²⁶. This strategy was generally applicable even without knowledge of the exact distribution of the observed effect size (such as in the RCCA), for which the confidence interval could be established based on variance estimated through methods such as bootstrap or jackknife.

Equivalence test for the first eigenvalue of RCCA. Due to the fact that correlations between RCCA components are forced non-negative, a test for the first eigenvalue

is equivalent to that for the correlation (for which the square is also known as Roy's largest root) between the first pair of components in the RCCA. We therefore only tested for inferiority in the corresponding equivalence test (that is, where Z_L was set as to $-\infty$ and Z_U (that is, Z_{Fisher} Fisher's r -to- z transformed correlation) was calculated as the inflated $Z_{\text{Fisher}0}$ between the first components of the RCCA under the null hypothesis (estimated through permutation) plus a small effect size, $q=0.1$, suggested by Cohen (that is, the difference between two Fisher-transformed correlations, known as Cohen's q ²⁷). The standard deviation (σ_z) of the observed Z_{Fisher} could be estimated through jackknife^{57,58}, and the corresponding t statistic for the one-tailed test could be calculated as $t = (Z_{\text{Fisher}} - 0.1 - Z_{\text{Fisher}0})/\sigma_z$.

Equivalence test for comparison of related correlations. Similar to above, the corresponding lower and upper equivalence bounds (ΔZ_L and ΔZ_U) of Fisher's r -to- z transformed correlation Z_{Fisher} were set as -0.1 and 0.1 , to represent a tiny effect size (Cohen's $D=0.1$). The variance (σ_z^2) of the observed Z_{Fisher} was estimated through jackknife, and the corresponding t statistics of one-tailed tests for the lower and upper bounds could be given as $(0.1 + Z_{\text{Fisher}})/\sigma_z$ and $(Z_{\text{Fisher}} - 0.1)/\sigma_z$, respectively.

Data distribution assumptions. Normality assumptions were made for all regression or correlation coefficients where either t statistic or F statistic test was applied. While the normality assumption was not formally tested, it has been guaranteed by the central limit theorem given the large sample in the present data⁶³. For the RCCA-related analyses, no assumption for data distribution was made as the null distributions were estimated directly through permutation.

Reporting Summary. Further information on research design is available in the Nature Research Reporting Summary linked to this article.

Data availability

IMAGEN data are available from a dedicated database: <https://imagen2.cea.fr>.

Code availability

Custom code that supports the findings of this study is available from the corresponding author upon request.

Received: 7 March 2019; Accepted: 28 February 2020;

Published online: 20 April 2020

References

- Castellanos, F. X., Sonuga-Barke, E. J., Milham, M. P. & Tannock, R. Characterizing cognition in ADHD: beyond executive dysfunction. *Trends Cogn. Sci.* **10**, 117–123 (2006).
- Blanken, L. M. et al. Cognitive functioning in children with internalising, externalising and dysregulation problems: a population-based study. *Eur. Child Adolesc. Psychiatry* **26**, 445–456 (2017).
- Shakoor, S., McGuire, P., Cardno, A. G., Freeman, D. & Ronald, A. A twin study exploring the association between childhood emotional and behaviour problems and specific psychotic experiences in a community sample of adolescents. *J. Child Psychol. Psychiatry* **59**, 565–573 (2018).
- Schumann, G. et al. The IMAGEN study: reinforcement-related behaviour in normal brain function and psychopathology. *Mol. Psychiatry* **15**, 1128–1139 (2010).
- Chen, J. E. & Glover, G. H. Erratum to: functional magnetic resonance imaging methods. *Neuropsychol. Rev.* **25**, 314 (2015).
- Nymberg, C. et al. Neural mechanisms of attention-deficit/hyperactivity disorder symptoms are stratified by MAOA genotype. *Biol. Psychiatry* **74**, 607–614 (2013).
- Dalley, J. W. & Robbins, T. W. Fractionating impulsivity: neuropsychiatric implications. *Nat. Rev. Neurosci.* **18**, 158–171 (2017).
- Schultz, W. Neuronal reward and decision signals: from theories to data. *Physiol. Rev.* **95**, 853–951 (2015).
- Aron, A. R., Robbins, T. W. & Poldrack, R. A. Inhibition and the right inferior frontal cortex: one decade on. *Trends Cogn. Sci.* **18**, 177–185 (2014).
- Quinlan, E. B. et al. Psychosocial stress and brain function in adolescent psychopathology. *Am. J. Psychiatry* **174**, 785–794 (2017).
- Adolphs, R. Cognitive neuroscience of human social behaviour. *Nat. Rev. Neurosci.* **4**, 165–178 (2003).
- Jia, T. et al. Neural basis of reward anticipation and its genetic determinants. *Proc. Natl Acad. Sci. USA* **113**, 3879–3884 (2016).
- Gerdes, A. B. et al. Emotional sounds modulate early neural processing of emotional pictures. *Front. Psychol.* **4**, 741 (2013).
- Serences, J. T. Value-based modulations in human visual cortex. *Neuron* **60**, 1169–1181 (2008).
- Pleger, B., Blankenburg, F., Ruff, C. C., Driver, J. & Dolan, R. J. Reward facilitates tactile judgments and modulates hemodynamic responses in human primary somatosensory cortex. *J. Neurosci.* **28**, 8161–8168 (2008).

16. Salimpoor, V. N. et al. Interactions between the nucleus accumbens and auditory cortices predict music reward value. *Science* **340**, 216–219 (2013).
17. Goodman, A., Lamping, D. L. & Ploubidis, G. B. When to use broader internalising and externalising subscales instead of the hypothesised five subscales on the strengths and difficulties questionnaire (SDQ): data from British parents, teachers and children. *J. Abnorm. Child Psychol.* **38**, 1179–1191 (2010).
18. Mumford, J. A. et al. Detecting network modules in fMRI time series: a weighted network analysis approach. *Neuroimage* **52**, 1465–1476 (2010).
19. Vinod, H. D. Canonical ridge and econometrics of joint production. *J. Econometrics* **4**, 147–166 (1976).
20. Knutson, B., Fong, G. W., Adams, C. M., Varner, J. L. & Hommer, D. Dissociation of reward anticipation and outcome with event-related fMRI. *Neuroreport* **12**, 3683–3687 (2001).
21. Bari, A. & Robbins, T. W. Inhibition and impulsivity: behavioral and neural basis of response control. *Prog. Neurobiol.* **108**, 44–79 (2013).
22. Grosbras, M. H. & Paus, T. Brain networks involved in viewing angry hands or faces. *Cereb. Cortex* **16**, 1087–1096 (2006).
23. Langfelder, P., Zhang, B. & Horvath, S. Defining clusters from a hierarchical cluster tree: the Dynamic Tree Cut package for R. *Bioinformatics* **24**, 719–720 (2008).
24. Bartels, M. et al. Childhood aggression and the co-occurrence of behavioural and emotional problems: results across ages 3–16 years from multiple raters in six cohorts in the EU-ACTION project. *Eur. Child Adolesc. Psychiatry* **27**, 1105–1121 (2018).
25. Kuhfeld, W. F. A note on Roy's largest root. *Psychometrika* **51**, 479–481 (1986).
26. Lakens, D. Equivalence tests: a practical primer for *t* tests, correlations, and meta-analyses. *Soc. Psychol. Personal Sci.* **8**, 355–362 (2017).
27. Cohen, J. *Statistical Power Analysis for the Behavioral Sciences* (L. Erlbaum Associates, 1988).
28. Krueger, R. F. et al. Progress in achieving quantitative classification of psychopathology. *World Psychiatry* **17**, 282–293 (2018).
29. Cuthbert, B. N. & Insel, T. R. Toward the future of psychiatric diagnosis: the seven pillars of RDoC. *BMC Med.* **11**, 126 (2013).
30. Pas, P., van den Munkhof, H. E., du Plessis, S. & Vink, M. Striatal activity during reactive inhibition is related to the expectation of stop-signals. *Neuroscience* **361**, 192–198 (2017).
31. Fox, P. T. & Friston, K. J. Distributed processing: distributed functions? *Neuroimage* **61**, 407–426 (2012).
32. Robinson, J. L., Laird, A. R., Glahn, D. C., Lovallo, W. R. & Fox, P. T. Metaanalytic connectivity modeling: delineating the functional connectivity of the human amygdala. *Hum. Brain Mapp.* **31**, 173–184 (2010).
33. Logothetis, N. K. What we can do and what we cannot do with fMRI. *Nature* **453**, 869–878 (2008).
34. Li, J. et al. Primary auditory cortex is required for anticipatory motor response. *Cereb. Cortex* **27**, 3254–3271 (2017).
35. Mountcastle, V. B., Lynch, J. C., Georgopoulos, A., Sakata, H. & Acuna, C. Posterior parietal association cortex of the monkey: command functions for operations within extrapersonal space. *J. Neurophysiol.* **38**, 871–908 (1975).
36. Rubia, K., Smith, A. B., Brammer, M. J. & Taylor, E. Temporal lobe dysfunction in medication-naïve boys with attention-deficit/hyperactivity disorder during attention allocation and its relation to response variability. *Biol. Psychiatry* **62**, 999–1006 (2007).
37. Swanson, J. M. et al. Etiologic subtypes of attention-deficit/hyperactivity disorder: brain imaging, molecular genetic and environmental factors and the dopamine hypothesis. *Neuropsychol. Rev.* **17**, 39–59 (2007).
38. Hobson, C. W., Scott, S. & Rubia, K. Investigation of cool and hot executive function in ODD/CD independently of ADHD. *J. Child Psychol. Psychiatry* **52**, 1035–1043 (2011).
39. Scheres, A., Oosterlaan, J. & Sergeant, J. A. Response inhibition in children with DSM-IV subtypes of AD/HD and related disruptive disorders: the role of reward. *Child Neuropsychol.* **7**, 172–189 (2001).
40. Burke, J. D., Waldman, I. & Lahey, B. B. Predictive validity of childhood oppositional defiant disorder and conduct disorder: implications for the DSM-V. *J. Abnorm. Psychol.* **119**, 739–751 (2010).
41. Spencer, T., Biederman, J. & Wilens, T. Attention-deficit/hyperactivity disorder and comorbidity. *Pediatr. Clin. North Am.* **46**, 915–927 (1999).
42. Jensen, P. S., Martin, D. & Cantwell, D. P. Comorbidity in ADHD: implications for research, practice, and DSM-V. *J. Am. Acad. Child Adolesc. Psychiatry* **36**, 1065–1079 (1997).
43. Heidebreder, R. ADHD symptomatology is best conceptualized as a spectrum: a dimensional versus unitary approach to diagnosis. *Atten. Defic. Hyperact. Disord.* **7**, 249–269 (2015).
44. Whelan, R. et al. Adolescent impulsivity phenotypes characterized by distinct brain networks. *Nat. Neurosci.* **15**, 920–925 (2012).
45. Goodman, R. Psychometric properties of the strengths and difficulties questionnaire. *J. Am. Acad. Child Adolesc. Psychiatry* **40**, 1337–1345 (2001).
46. Herjanic, B. & Reich, W. Development of a structured psychiatric interview for children: agreement between child and parent on individual symptoms. *J. Abnorm. Child Psychol.* **25**, 21–31 (1997).
47. Goodman, R., Ford, T., Richards, H., Gatward, R. & Meltzer, H. The development and well-being assessment: description and initial validation of an integrated assessment of child and adolescent psychopathology. *J. Child Psychol. Psychiatry* **41**, 645–655 (2000).
48. Ernst, M. et al. Choice selection and reward anticipation: an fMRI study. *Neuropsychologia* **42**, 1585–1597 (2004).
49. Cooney, R. E., Atlas, L. Y., Joormann, J., Eugene, F. & Gotlib, I. H. Amygdala activation in the processing of neutral faces in social anxiety disorder: is neutral really neutral? *Psychiatry Res.* **148**, 55–59 (2006).
50. Passamonti, L. et al. Neural abnormalities in early-onset and adolescence-onset conduct disorder. *Arch. Gen. Psychiatry* **67**, 729–738 (2010).
51. Pardini, D. A. & Phillips, M. Neural responses to emotional and neutral facial expressions in chronically violent men. *J. Psychiatry Neurosci.* **35**, 390–398 (2010).
52. Gan, G. et al. Alcohol-induced impairment of inhibitory control is linked to attenuated brain responses in right fronto-temporal cortex. *Biol. Psychiatry* **76**, 698–707 (2014).
53. Langfelder, P. & Horvath, S. WGCNA: an R package for weighted correlation network analysis. *BMC Bioinformatics* **9**, 559 (2008).
54. Combes, S. et al. Relationships between sensory and physicochemical measurements in meat of rabbit from three different breeding systems using canonical correlation analysis. *Meat Sci.* **80**, 835–841 (2008).
55. Leurgans, S. E., Moyeed, R. A. & Silverman, B. W. Canonical correlation-analysis when the data are curves. *J. R. Stat. Soc. B Met.* **55**, 725–740 (1993).
56. Sherry, A. & Henson, R. K. Conducting and interpreting canonical correlation analysis in personality research: a user-friendly primer. *J. Pers. Assess.* **84**, 37–48 (2005).
57. Efron, B. & Stein, C. The jackknife estimate of variance. *Ann. Stat.* **9**, 586–596 (1981).
58. Bulik-Sullivan, B. et al. An atlas of genetic correlations across human diseases and traits. *Nat. Genet.* **47**, 1236–1241 (2015).
59. Fisher, R. A. On the probable error of a coefficient of correlation deduced from a small sample. *Metron* **1**, 3–32 (1921).
60. Dunn, O. J. & Clark, V. Correlation coefficients measured on the same individuals. *J. Am. Stat. Assoc.* **64**, 366–377 (1969).
61. Steiger, J. H. Tests for comparing elements of a correlation matrix. *Psychol. Bull.* **87**, 245–251 (1980).
62. Meng, X.-L., Rosenthal, R. & Rubin, D. B. Comparing correlated correlation coefficients. *Psychol. Bull.* **111**, 172–175 (1992).
63. Lumley, T., Diehr, P., Emerson, S. & Chen, L. The importance of the normality assumption in large public health data sets. *Annu. Rev. Public Health* **23**, 151–169 (2002).

Acknowledgements

This work received support from the following sources: the European Union-funded FP6 Integrated Project IMAGEN (reinforcement-related behaviour in normal brain function and psychopathology; LSHM-CT-2007-037286), the Horizon 2020-funded ERC Advanced Grant 'STRATIFY' (brain network-based stratification of reinforcement-related disorders; 695313), National Natural Science Foundation of China (81801773 and 81873909), the Shanghai Pujiang Project (18PJ1400900), ERANID (understanding the interplay between cultural, biological and subjective factors in drug use pathways; PR-ST-0416-10004), BRIDGET (JPND brain imaging, cognition, dementia and next generation GENomics; MR/N027558/1), the Human Brain Project (SGA 2, 785907, and SGA 3, 945539), the FP7 project MATRICS (603016), the Medical Research Council Grant 'c-VEDA' (consortium on vulnerability to externalizing disorders and addictions; MR/N000390/1), the National Institute of Health (NIH) (R01DA049238, A decentralized macro and micro gene-by-environment interaction analysis of substance use behavior and its brain biomarkers), the National Institute for Health Research Biomedical Research Centre at South London and Maudsley NHS Foundation Trust and King's College London, the Bundesministerium für Bildung und Forschung (grants 01GS08152 and 01EV0711 and Forschungsnetz AERIAL 01EE1406A and 01EE1406B), the Deutsche Forschungsgemeinschaft (DFG grants SM 80/7-2, SFB 940, TRR 265 and NE 1383/14-1), the Medical Research Foundation and Medical Research Council (grants MR/R00465X/1 and MR/S020306/1), the National Institutes of Health (NIH)-funded ENIGMA (grants 5U54EB020403-05 and 1R56AG058854-01). Further support was provided by grants from: ANR ANR-12-SAMA-0004, AAPG2019 - GeBra), the Eranet Neuron (AF12-NEUR0008-01 - WM2NA and ANR-18-NEUR00002-01 - ADORé), the Fondation de France (00081242), the Fondation pour la Recherche Médicale (DPA20140629802), the Mission Interministérielle de Lutte Contre les Drogues et les Conduites Addictives (MILDECA), the Assistance-Publique – Hôpitaux de Paris et INSERM (interface grant), Paris Sud University IDEX 2012, the Fondation de l'avenir (grant AP-RM-17-013), the Fédération pour la Recherche sur le Cerveau, the National Institutes of Health, Science Foundation Ireland (16/ERC/D/3797) and U.S.A. (Axon, Testosterone and Mental Health during Adolescence; RO1 MH085772-01A1), and by NIH Consortium grant U54 EB020403 (supported by a cross-NIH alliance that funds Big Data to Knowledge Centres of Excellence), the 111 Project (B18015), the National Key Research and Development

Program of China (2018YFC0910503 and 2018YFC1312900), the NSFC (81930095 and 91630314), The Key Project of Shanghai Science and Technology Innovation Plan (16JC1420402), the Shanghai Municipal Science and Technology Major Project (2018SHZDZX01) and Zhangjiang Lab. The funders had no role in study design, data collection and analysis, decision to publish or preparation of the manuscript.

Author contributions

G.S. and T.J. designed the study. T.J. and G.S. wrote the manuscript. A.I., E.B.Q., N.T., Q.L. and B.F. edited the first draft. All authors critically reviewed the manuscript. T.B., G.J.B., A.L.W.B., U.B., C.B., S.D., J.F., H.F., A.G., H.G., P.G., A.H., B.I., J.-L.M., M.-L.P.M., F.N., T.P., L.P., J.H.F., M.N.S., H.W., R.W. and G.S. were the principal investigators. E.B.Q., T.B., G.J.B., A.L.W.B., U.B., C.B., H.F., A.G., H.G., P.G., A.H., B.I., J.-L.M., M.-L.P.M., F.N., D.P.O., T.P., L.P., J.H.F., M.N.S., H.W., R.W. and G.S. acquired the data. T.J. and A.I. analysed the data.

Competing interests

T.B. served in an advisory or consultancy role for Lundbeck, Medice, Neurim Pharmaceuticals, Oberberg and Shire. He received conference support or speaker's fees

from Lilly, Medice, Novartis and Shire. He has been involved in clinical trials conducted by Shire and Vifor Pharma. He received royalties from Hogrefe, Kohlhammer, CIP Medien and Oxford University Press. The present work is unrelated to the above grants and relationships. G.J.B. has received honoraria from General Electric Healthcare for teaching on scanner programming courses. The other authors declare no competing interests.

Additional information

Extended data is available for this paper at <https://doi.org/10.1038/s41562-020-0846-5>.

Supplementary information is available for this paper at <https://doi.org/10.1038/s41562-020-0846-5>.

Correspondence and requests for materials should be addressed to T.J. or G.S.

Reprints and permissions information is available at www.nature.com/reprints.

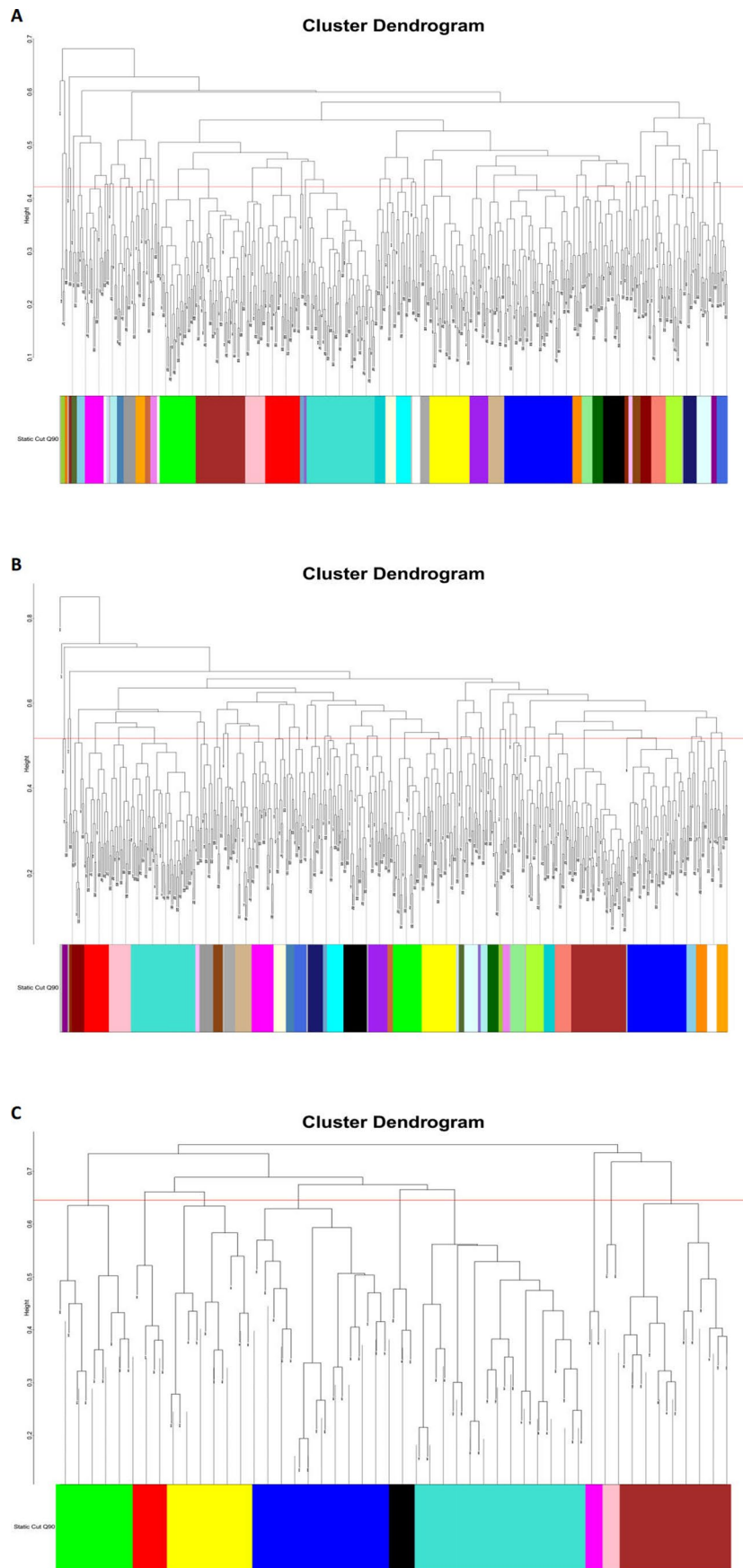
Publisher's note Springer Nature remains neutral with regard to jurisdictional claims in published maps and institutional affiliations.

Editor recognition statement: Primary Handling Editor: Marike Schiffer.

© The Author(s), under exclusive licence to Springer Nature Limited 2020

IMAGEN Consortium

Tianye Jia^{1,2,3,4}, Alex Ing³, Erin Burke Quinlan³, Biondo Francesca⁵, Tobias Banaschewski⁶, Gareth J. Barker⁷, Arun L. W. Bokde⁸, Uli Bromberg⁹, Christian Büchel⁹, Sylvane Desrivières³, Herta Flor^{14,15}, Hugh Garavan¹⁷, Penny Gowland¹⁸, Andreas Heinz¹⁹, Bernd Ittermann²⁰, Jean-Luc Martinot^{21,22}, Frauke Nees^{6,14}, Dimitri Papadopoulos Orfanos¹⁶, Tomáš Paus²⁴, Luise Poustka²⁵, Juliane H. Fröhner²⁶, Michael N. Smolka²⁶, Henrik Walter¹⁹, Robert Whelan²⁷ and Gunter Schumann^{1,3,28}



Extended Data Fig. 1 | Dendrograms of hierarchical clustering for WVCNA nodes. Dendrogram trees and static cut at 90% quantile of height of branches for (A) MID, (B) SST and (C) EFT nodes from WVCNA.

	Region of Interests		Presence in fMRI Tasks		
			MID	EFT	SST
Prefrontal Cortex	dorsal lateral frontal cortex	anterior	L/R		L/R
		posterior			L/R
	orbital frontal cortex	dorsal	L/R		L/R
		ventral	L/R	medial	L/R
	inferior frontal cortex	orbito-triangular		L/R	R L/R
Insula			L/R		L/R
Motor and Somatosensory Cortex	premotor cortex	superior	L/R		L/R
		inferior	L/R	R	L/R
		Rolandic operculum	L/R		
		Inferior frontal junction	L/R	L/R	L/R
	supplementary motor area		highest in SMA	dorsal	highest in pre-SMA
primary motor cortex		L/R		L/R	
primary somatosensory cortex	superior	L/R			
	inferior			L/R	
Cingulate Cortex	anterior cingulate cortex		L/R		L/R
	posterior cingulate cortex	posterior dorsal		R	
		posterior ventral	L/R		L/R
Subcortical Area	striatum	dorsal	L/R		
		ventral	L/R		L/R
	thalamus	dorsal	L/R		L/R
	amygdala	ventral		L/R	
		dorsal	L/R	L/R	
Temporal Lobe	pole	ventral		R	R
		anterior		R	L/R
	superior temporal sulcus	middle		L/R	L/R
		posterior		L/R	L/R
	primary auditory cortex		L/R		
	fusiform gyrus		posterior L/R	L/R	L/R
	parahippocampal gyrus		L/R		L/R
	temporo-occipital junction		L/R		L/R
	inferior temporal gyrus	posterior			R
	Parietal Lobe	precuneus	dorsal	L/R	
intra-parietal sulcus			L/R		L/R
temporo-parietal junction		supramarginal gyrus	L/R		L/R
		angular gyrus			
parietal-occipital junction			L/R		L/R
Occipital Lobe	pole		L/R	L/R	L/R
			L/R		L/R
	lingual gyrus		L/R	L/R	L/R
	occipital gyri	superior	L/R		L/R
		middle	L/R		L/R
		inferior	L/R	L/R	L/R
	temporo-parietal-occipital junction			L/R	L/R
parietal-occipital junction		L/R		L/R	
Cerebellum	quadriangular lobule	anterior	L/R		
		posterior	L/R		
	semilunar lobule	superior	L/R		
		Inferior	L/R	posterior L	anterior L/R; posterior L
	biventral lobule		L/R	middle L	anterior L; posterior L/R
	cerebellar vermis	lingula			medial
		central	medial		
		culmen	medial		
declive		medial			
folium		medial			
tuber		medial	medial	medial	
pyramis	medial				
uvula	medial	medial			
nodule				medial	

Extended Data Fig. 2 | Overlapped functional brain regions. Overlapped Functional Brain Regions (Cohen's D > 0.30) Identified across All Three Tasks.

A

Regulation Parameter	fMRI	η^2 [90% CIs]		
		ADHD	ODD/CD	All
0.1	MID	0.365 [0.335,0.394]	0.338 [0.307,0.370]	0.579 [0.551,0.607]
	SST	0.352 [0.320,0.384]	0.343 [0.309,0.376]	0.573 [0.543,0.603]
	EFT	0.089 [0.068,0.110]	0.092 [0.071,0.112]	0.175 [0.148,0.203]
	All_fMRI			0.854 [0.839,0.869]
0.2	MID	0.270 [0.246,0.294]	0.254 [0.229,0.280]	0.454 [0.428,0.479]
	SST	0.265 [0.238,0.292]	0.262 [0.234,0.290]	0.454 [0.425,0.483]
	EFT	0.069 [0.052,0.085]	0.072 [0.056,0.088]	0.137 [0.115,0.160]
	All_fMRI			0.744 [0.724,0.763]
0.3	MID	0.211 [0.191,0.232]	0.201 [0.179,0.223]	0.367 [0.344,0.390]
	SST	0.210 [0.186,0.233]	0.210 [0.186,0.234]	0.371 [0.345,0.398]
	EFT	0.055 [0.042,0.069]	0.058 [0.045,0.072]	0.112 [0.093,0.130]
	All_fMRI			0.646 [0.624,0.668]
0.4	MID	0.171 [0.153,0.189]	0.164 [0.145,0.183]	0.304 [0.283,0.325]
	SST	0.172 [0.151,0.192]	0.174 [0.153,0.195]	0.310 [0.286,0.335]
	EFT	0.046 [0.034,0.058]	0.048 [0.037,0.060]	0.093 [0.077,0.109]
	All_fMRI			0.564 [0.542,0.587]
0.5	MID	0.143 [0.127,0.158]	0.137 [0.121,0.154]	0.257 [0.238,0.276]
	SST	0.144 [0.126,0.162]	0.147 [0.128,0.166]	0.264 [0.242,0.287]
	EFT	0.039 [0.029,0.049]	0.041 [0.031,0.051]	0.079 [0.065,0.093]
	All_fMRI			0.496 [0.474,0.518]

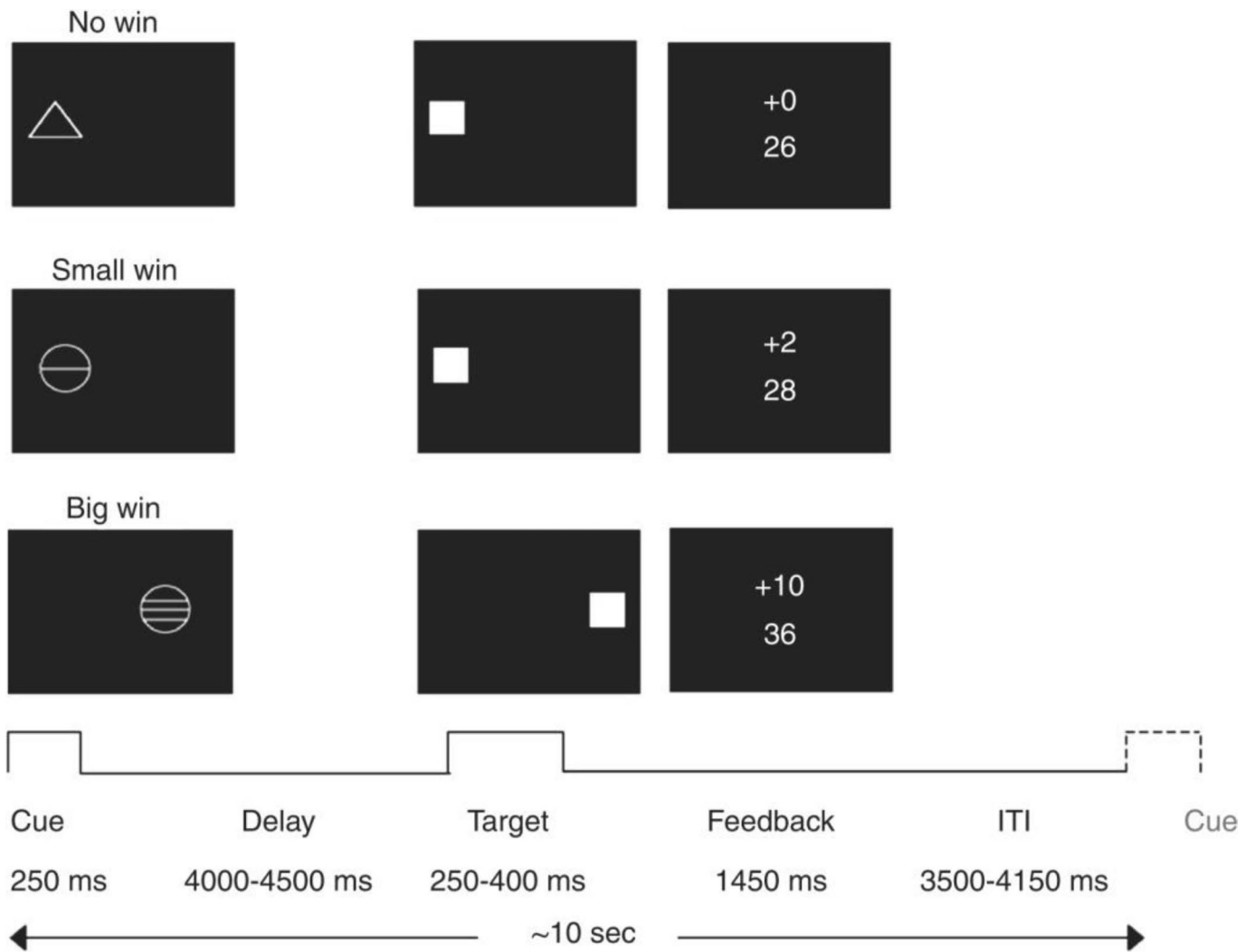
B

Regulation Parameter	fMRI	P-values		
		ADHD	ODD/CD	All
0.1	MID	0.029	0.203	0.036
	SST	0.003	0.003	<0.001
	EFT	0.634	0.294	0.392
	All_fMRI			<0.001
0.2	MID	0.029	0.211	0.038
	SST	0.005	0.004	<0.001
	EFT	0.594	0.301	0.291
	All_fMRI			<0.001
0.3	MID	0.031	0.220	0.039
	SST	<0.001	<0.001	<0.001
	EFT	0.481	0.300	0.252
	All_fMRI			<0.001
0.4	MID	0.034	0.224	0.044
	SST	0.002	0.003	<0.001
	EFT	0.422	0.287	0.228
	All_fMRI			<0.001
0.5	MID	0.035	0.237	0.036
	SST	0.001	0.002	<0.001
	EFT	0.406	0.285	0.197
	All_fMRI			<0.001

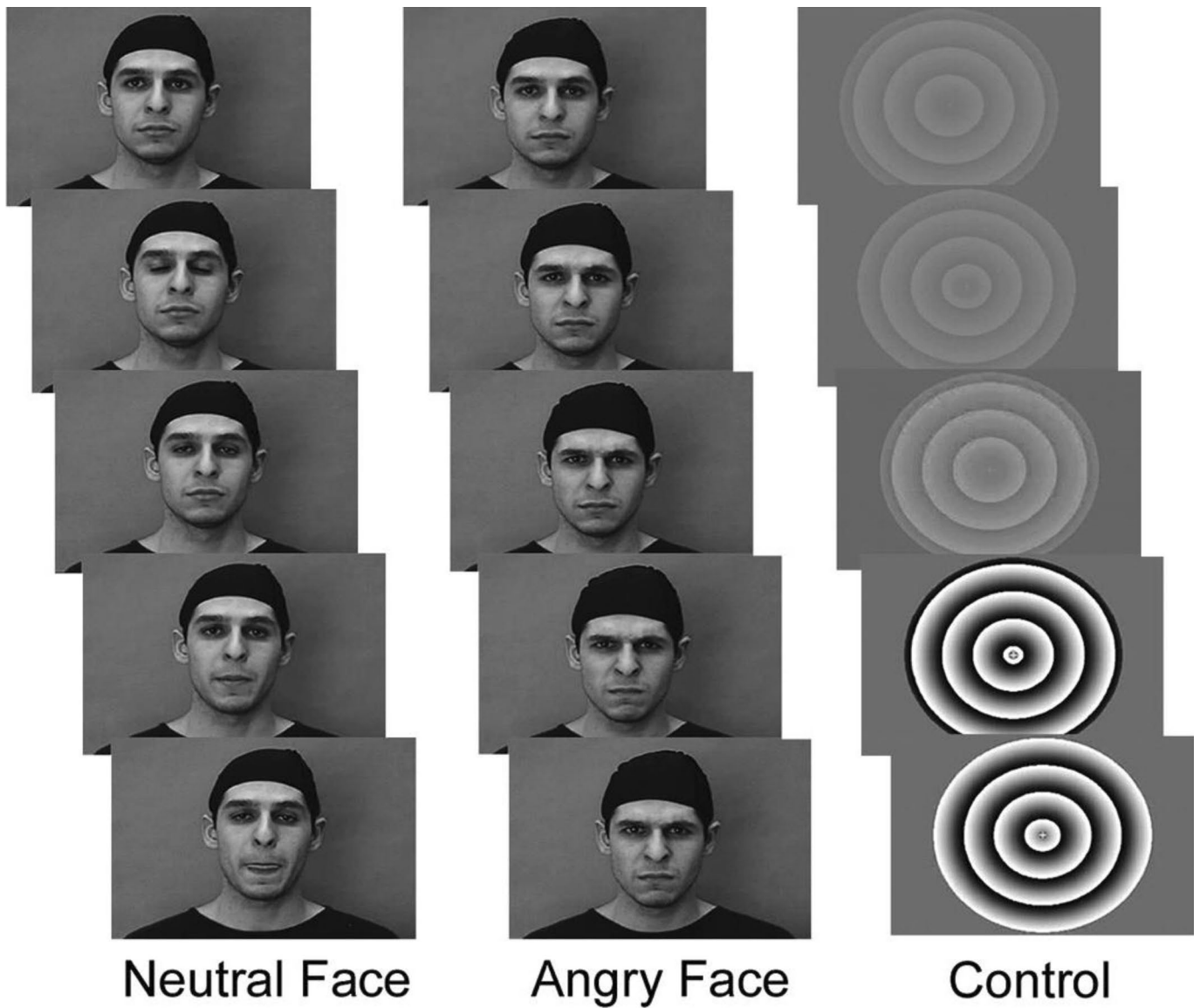
Extended Data Fig. 3 | Extended RCCA results between fMRI and externalizing behaviours. RCCA results between fMRI and externalising behaviours based on 1000 Permutation with predefined Regulation Parameters: A. The Effect Size (η^2) and Confidence Intervals; B. P-values.

Regulation Parameter	fMRI	Internalising Behaviours	
		P-value	η^2 [90% CIs]
0.1	MID	0.907	0.316 [0.286,0.345]
	SST	0.182	0.324 [0.294,0.354]
	EFT	0.808	0.083 [0.063,0.102]
	All_fMRI	0.786	0.574 [0.547,0.602]
0.2	MID	0.913	0.240 [0.216,0.264]
	SST	0.230	0.248 [0.223,0.273]
	EFT	0.797	0.066 [0.050,0.081]
	All_fMRI	0.842	0.463 [0.437,0.489]
0.3	MID	0.929	0.191 [0.170,0.211]
	SST	0.310	0.198 [0.177,0.219]
	EFT	0.796	0.054 [0.041,0.067]
	All_fMRI	0.870	0.383 [0.359,0.407]
0.4	MID	0.940	0.156 [0.139,0.174]
	SST	0.320	0.163 [0.145,0.181]
	EFT	0.785	0.045 [0.034,0.056]
	All_fMRI	0.887	0.323 [0.302,0.344]
0.5	MID	0.945	0.131 [0.116,0.147]
	SST	0.402	0.137 [0.121,0.152]
	EFT	0.775	0.039 [0.029,0.048]
	All_fMRI	0.907	0.277 [0.257,0.296]

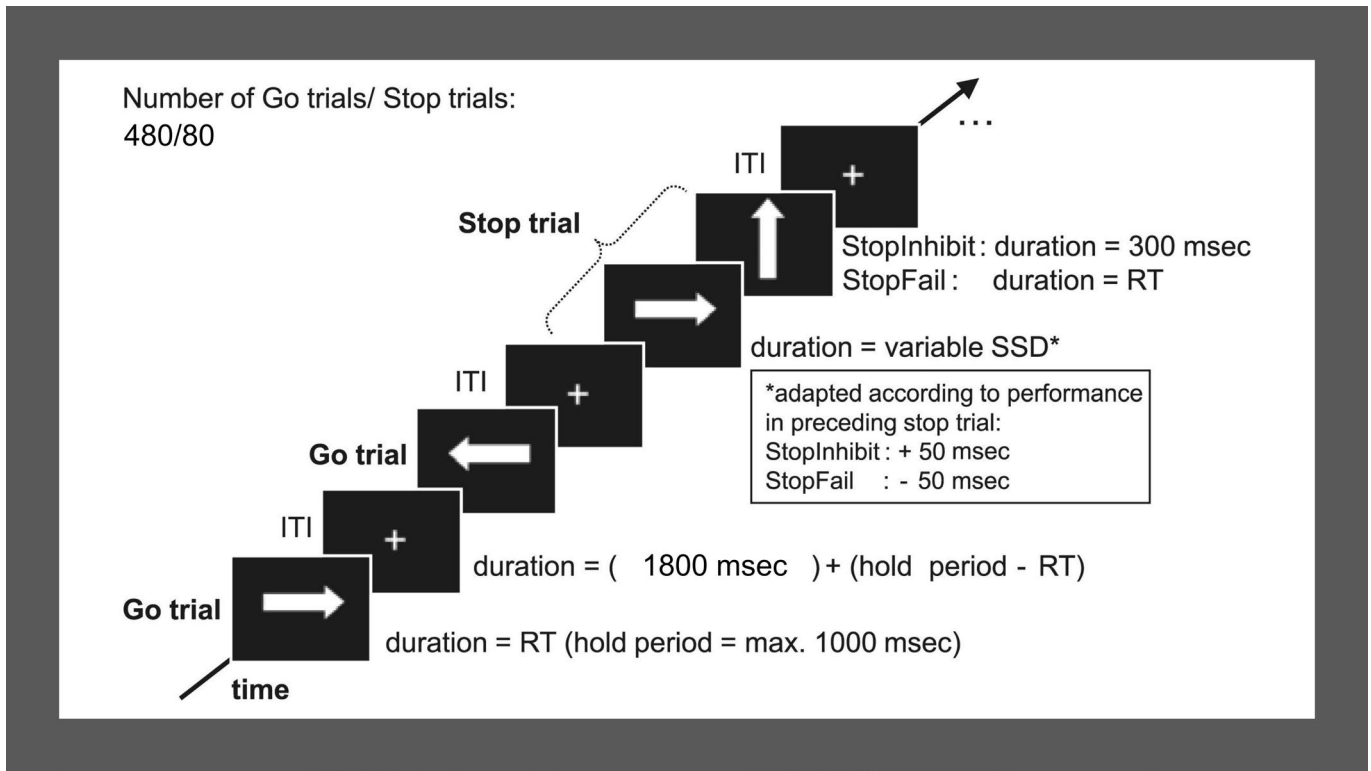
Extended Data Fig. 4 | Extended RCCA results between fMRI and internalizing behaviours. RCCA results between fMRI and internalising behaviours based on 1000 Permutation with predefined regulation parameters.



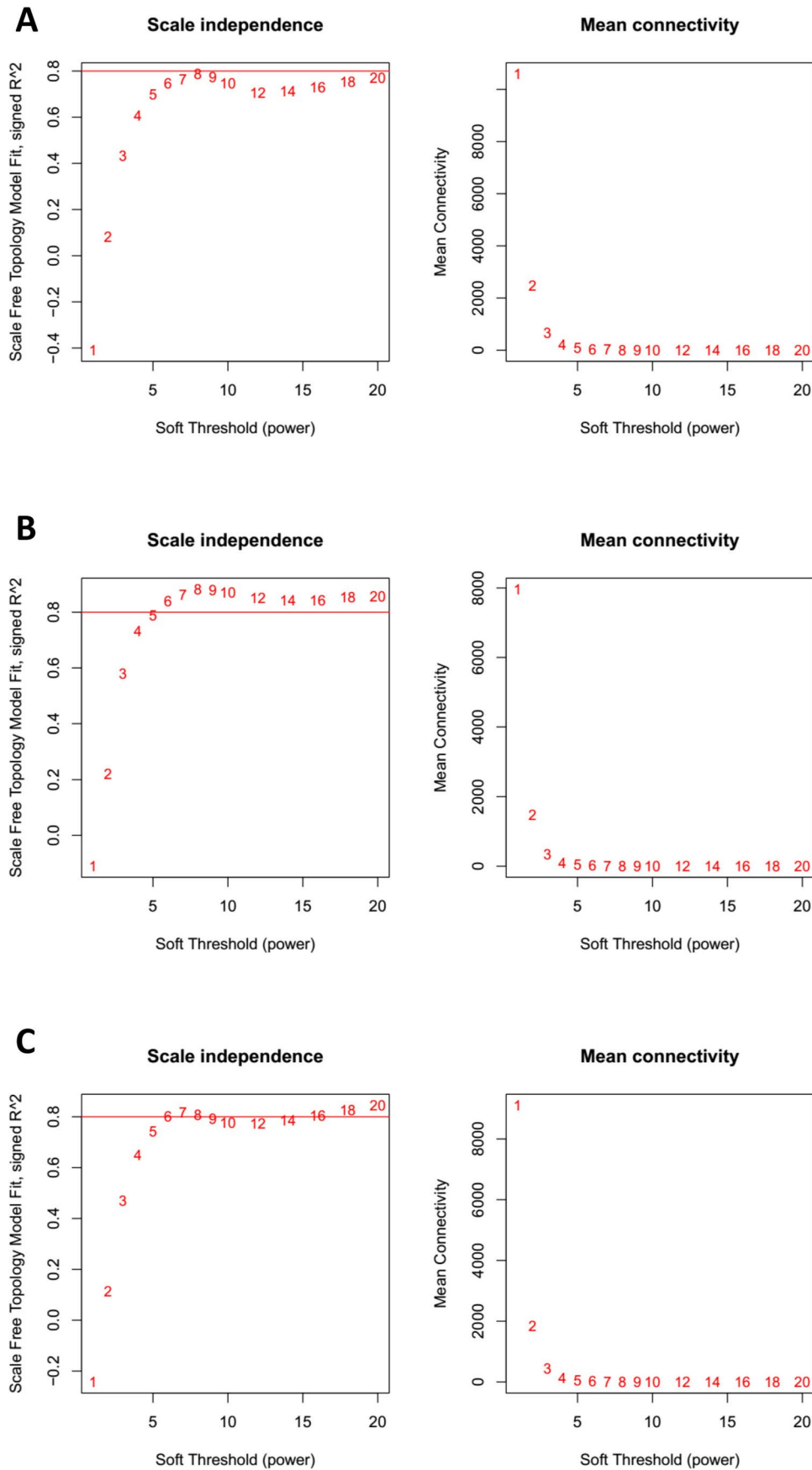
Extended Data Fig. 5 | The design of monetary incentive delay (MID) task. The figure of experimental paradigm was adapted from a previous publication⁶.



Extended Data Fig. 6 | The design of emotional face task (EFT). The figure of experimental paradigm was adapted from a previous publication²².



Extended Data Fig. 7 | The design of stop signal task (SST). The figure of experimental paradigm was adapted from a previous publication⁵².



Extended Data Fig. 8 | Plot of soft-threshold for MID (A), EFT (B) and SST (C). The soft-thresholds were picked as 7 for MID, 8 for EFT and 7 for SST.

Reporting Summary

Nature Research wishes to improve the reproducibility of the work that we publish. This form provides structure for consistency and transparency in reporting. For further information on Nature Research policies, see [Authors & Referees](#) and the [Editorial Policy Checklist](#).

Statistics

For all statistical analyses, confirm that the following items are present in the figure legend, table legend, main text, or Methods section.

n/a Confirmed

- | | | |
|-------------------------------------|-------------------------------------|--|
| <input type="checkbox"/> | <input checked="" type="checkbox"/> | The exact sample size (n) for each experimental group/condition, given as a discrete number and unit of measurement |
| <input type="checkbox"/> | <input checked="" type="checkbox"/> | A statement on whether measurements were taken from distinct samples or whether the same sample was measured repeatedly |
| <input type="checkbox"/> | <input checked="" type="checkbox"/> | The statistical test(s) used AND whether they are one- or two-sided
<i>Only common tests should be described solely by name; describe more complex techniques in the Methods section.</i> |
| <input type="checkbox"/> | <input checked="" type="checkbox"/> | A description of all covariates tested |
| <input type="checkbox"/> | <input checked="" type="checkbox"/> | A description of any assumptions or corrections, such as tests of normality and adjustment for multiple comparisons |
| <input type="checkbox"/> | <input checked="" type="checkbox"/> | A full description of the statistical parameters including central tendency (e.g. means) or other basic estimates (e.g. regression coefficient) AND variation (e.g. standard deviation) or associated estimates of uncertainty (e.g. confidence intervals) |
| <input type="checkbox"/> | <input checked="" type="checkbox"/> | For null hypothesis testing, the test statistic (e.g. F , t , r) with confidence intervals, effect sizes, degrees of freedom and P value noted
<i>Give P values as exact values whenever suitable.</i> |
| <input checked="" type="checkbox"/> | <input type="checkbox"/> | For Bayesian analysis, information on the choice of priors and Markov chain Monte Carlo settings |
| <input type="checkbox"/> | <input checked="" type="checkbox"/> | For hierarchical and complex designs, identification of the appropriate level for tests and full reporting of outcomes |
| <input type="checkbox"/> | <input checked="" type="checkbox"/> | Estimates of effect sizes (e.g. Cohen's d , Pearson's r), indicating how they were calculated |

Our web collection on [statistics for biologists](#) contains articles on many of the points above.

Software and code

Policy information about [availability of computer code](#)

Data collection

Psytool platform was used to collect data for both SDQ and DAWBA assessment.

Data analysis

All statistical analyses were conducted in the R programme. The R package WGCNA was used to conduct WGCNA of task-based fMRI Data. Preprocessing and first level analyses of task-based fMRI data were conducted in SPM8.

For manuscripts utilizing custom algorithms or software that are central to the research but not yet described in published literature, software must be made available to editors/reviewers. We strongly encourage code deposition in a community repository (e.g. GitHub). See the Nature Research [guidelines for submitting code & software](#) for further information.

Data

Policy information about [availability of data](#)

All manuscripts must include a [data availability statement](#). This statement should provide the following information, where applicable:

- Accession codes, unique identifiers, or web links for publicly available datasets
- A list of figures that have associated raw data
- A description of any restrictions on data availability

IMAGEN data are available from a dedicated database: <https://imagen.cea.fr>.

Field-specific reporting

Please select the one below that is the best fit for your research. If you are not sure, read the appropriate sections before making your selection.

- Life sciences Behavioural & social sciences Ecological, evolutionary & environmental sciences

Life sciences study design

All studies must disclose on these points even when the disclosure is negative.

Sample size	In total 1506 individuals with complete data of fMRI or behaviours were involved in the present study. This sample size is sufficiently to detect effect size as little as 2% of variance with a statistical power 95% at significance level 0.0001.
Data exclusions	Individuals with incomplete data across fMRI and behaviours were excluded in the CCA analyses. Also, individuals were excluded during the WVCNA procedure if they were detected as outliers, i.e. highly different from the rest of the sample.
Replication	No replication was conducted due to the unique character of this sample.
Randomization	As a population study, no randomization was conducted. However, covariates (i.e. gender, research sites and handedness) were regressed out before the conduct of CCA from all fMRI and behaviour data.
Blinding	As a population study, no blinding was conducted.

Behavioural & social sciences study design

All studies must disclose on these points even when the disclosure is negative.

Study description	<i>Briefly describe the study type including whether data are quantitative, qualitative, or mixed-methods (e.g. qualitative cross-sectional, quantitative experimental, mixed-methods case study).</i>
Research sample	<i>State the research sample (e.g. Harvard university undergraduates, villagers in rural India) and provide relevant demographic information (e.g. age, sex) and indicate whether the sample is representative. Provide a rationale for the study sample chosen. For studies involving existing datasets, please describe the dataset and source.</i>
Sampling strategy	<i>Describe the sampling procedure (e.g. random, snowball, stratified, convenience). Describe the statistical methods that were used to predetermine sample size OR if no sample-size calculation was performed, describe how sample sizes were chosen and provide a rationale for why these sample sizes are sufficient. For qualitative data, please indicate whether data saturation was considered, and what criteria were used to decide that no further sampling was needed.</i>
Data collection	<i>Provide details about the data collection procedure, including the instruments or devices used to record the data (e.g. pen and paper, computer, eye tracker, video or audio equipment) whether anyone was present besides the participant(s) and the researcher, and whether the researcher was blind to experimental condition and/or the study hypothesis during data collection.</i>
Timing	<i>Indicate the start and stop dates of data collection. If there is a gap between collection periods, state the dates for each sample cohort.</i>
Data exclusions	<i>If no data were excluded from the analyses, state so OR if data were excluded, provide the exact number of exclusions and the rationale behind them, indicating whether exclusion criteria were pre-established.</i>
Non-participation	<i>State how many participants dropped out/declined participation and the reason(s) given OR provide response rate OR state that no participants dropped out/declined participation.</i>
Randomization	<i>If participants were not allocated into experimental groups, state so OR describe how participants were allocated to groups, and if allocation was not random, describe how covariates were controlled.</i>

Ecological, evolutionary & environmental sciences study design

All studies must disclose on these points even when the disclosure is negative.

Study description	<i>Briefly describe the study. For quantitative data include treatment factors and interactions, design structure (e.g. factorial, nested, hierarchical), nature and number of experimental units and replicates.</i>
Research sample	<i>Describe the research sample (e.g. a group of tagged <i>Passer domesticus</i>, all <i>Stenocereus thurberi</i> within Organ Pipe Cactus National Monument), and provide a rationale for the sample choice. When relevant, describe the organism taxa, source, sex, age range and any manipulations. State what population the sample is meant to represent when applicable. For studies involving existing datasets, describe the data and its source.</i>
Sampling strategy	<i>Note the sampling procedure. Describe the statistical methods that were used to predetermine sample size OR if no sample-size calculation was performed, describe how sample sizes were chosen and provide a rationale for why these sample sizes are sufficient.</i>
Data collection	<i>Describe the data collection procedure, including who recorded the data and how.</i>

Timing and spatial scale *Indicate the start and stop dates of data collection, noting the frequency and periodicity of sampling and providing a rationale for these choices. If there is a gap between collection periods, state the dates for each sample cohort. Specify the spatial scale from which the data are taken*

Data exclusions *If no data were excluded from the analyses, state so OR if data were excluded, describe the exclusions and the rationale behind them, indicating whether exclusion criteria were pre-established.*

Reproducibility *Describe the measures taken to verify the reproducibility of experimental findings. For each experiment, note whether any attempts to repeat the experiment failed OR state that all attempts to repeat the experiment were successful.*

Randomization *Describe how samples/organisms/participants were allocated into groups. If allocation was not random, describe how covariates were controlled. If this is not relevant to your study, explain why.*

Blinding *Describe the extent of blinding used during data acquisition and analysis. If blinding was not possible, describe why OR explain why blinding was not relevant to your study.*

Did the study involve field work? Yes No

Field work, collection and transport

Field conditions *Describe the study conditions for field work, providing relevant parameters (e.g. temperature, rainfall).*

Location *State the location of the sampling or experiment, providing relevant parameters (e.g. latitude and longitude, elevation, water depth).*

Access and import/export *Describe the efforts you have made to access habitats and to collect and import/export your samples in a responsible manner and in compliance with local, national and international laws, noting any permits that were obtained (give the name of the issuing authority, the date of issue, and any identifying information).*

Disturbance *Describe any disturbance caused by the study and how it was minimized.*

Reporting for specific materials, systems and methods

We require information from authors about some types of materials, experimental systems and methods used in many studies. Here, indicate whether each material, system or method listed is relevant to your study. If you are not sure if a list item applies to your research, read the appropriate section before selecting a response.

Materials & experimental systems

n/a	Involved in the study
<input checked="" type="checkbox"/>	<input type="checkbox"/> Antibodies
<input checked="" type="checkbox"/>	<input type="checkbox"/> Eukaryotic cell lines
<input checked="" type="checkbox"/>	<input type="checkbox"/> Palaeontology
<input checked="" type="checkbox"/>	<input type="checkbox"/> Animals and other organisms
<input type="checkbox"/>	<input checked="" type="checkbox"/> Human research participants
<input checked="" type="checkbox"/>	<input type="checkbox"/> Clinical data

Methods

n/a	Involved in the study
<input checked="" type="checkbox"/>	<input type="checkbox"/> ChIP-seq
<input checked="" type="checkbox"/>	<input type="checkbox"/> Flow cytometry
<input type="checkbox"/>	<input checked="" type="checkbox"/> MRI-based neuroimaging

Antibodies

Antibodies used *Describe all antibodies used in the study; as applicable, provide supplier name, catalog number, clone name, and lot number.*

Validation *Describe the validation of each primary antibody for the species and application, noting any validation statements on the manufacturer's website, relevant citations, antibody profiles in online databases, or data provided in the manuscript.*

Eukaryotic cell lines

Policy information about [cell lines](#)

Cell line source(s) *State the source of each cell line used.*

Authentication *Describe the authentication procedures for each cell line used OR declare that none of the cell lines used were authenticated.*

Mycoplasma contamination *Confirm that all cell lines tested negative for mycoplasma contamination OR describe the results of the testing for mycoplasma contamination OR declare that the cell lines were not tested for mycoplasma contamination.*

Commonly misidentified lines (See [ICLAC](#) register) *Name any commonly misidentified cell lines used in the study and provide a rationale for their use.*

Palaeontology

Specimen provenance	<i>Provide provenance information for specimens and describe permits that were obtained for the work (including the name of the issuing authority, the date of issue, and any identifying information).</i>
Specimen deposition	<i>Indicate where the specimens have been deposited to permit free access by other researchers.</i>
Dating methods	<i>If new dates are provided, describe how they were obtained (e.g. collection, storage, sample pretreatment and measurement), where they were obtained (i.e. lab name), the calibration program and the protocol for quality assurance OR state that no new dates are provided.</i>

Tick this box to confirm that the raw and calibrated dates are available in the paper or in Supplementary Information.

Animals and other organisms

Policy information about [studies involving animals](#); [ARRIVE guidelines](#) recommended for reporting animal research

Laboratory animals	<i>For laboratory animals, report species, strain, sex and age OR state that the study did not involve laboratory animals.</i>
Wild animals	<i>Provide details on animals observed in or captured in the field; report species, sex and age where possible. Describe how animals were caught and transported and what happened to captive animals after the study (if killed, explain why and describe method; if released, say where and when) OR state that the study did not involve wild animals.</i>
Field-collected samples	<i>For laboratory work with field-collected samples, describe all relevant parameters such as housing, maintenance, temperature, photoperiod and end-of-experiment protocol OR state that the study did not involve samples collected from the field.</i>
Ethics oversight	<i>Identify the organization(s) that approved or provided guidance on the study protocol, OR state that no ethical approval or guidance was required and explain why not.</i>

Note that full information on the approval of the study protocol must also be provided in the manuscript.

Human research participants

Policy information about [studies involving human research participants](#)

Population characteristics	Healthy Caucasian adolescents at age 14 were recruited from middle-class school across Europe. Of the 1506 participants investigated in this study, clinical DAWBA ratings are available from 1190 individuals. Of these individuals 131 have one or more diagnoses: 33 individuals were diagnosed with ADHD, 59 with emotional problems, 12 with anxiety (general + other) and 33 with depression (major + other)
Recruitment	Healthy Caucasian adolescents at age 14 were recruited from middle-class school from multiple sites across Europe (London, Nottingham, Dublin, Paris, Manhanm, Berlin, Dresden, Humberg).
Ethics oversight	The IMAGEN Study was approved by local ethics research committees at each research site: King's College London, University of Nottingham, Trinity College Dublin, University of Heidelberg, Technische Universität Dresden, Commissariat à l'Énergie Atomique et aux Énergies Alternatives, and University Medical Center. Informed consent was sought from all participants and a parent/guardian of each participant.

Note that full information on the approval of the study protocol must also be provided in the manuscript.

Clinical data

Policy information about [clinical studies](#)

All manuscripts should comply with the ICMJE [guidelines for publication of clinical research](#) and a completed [CONSORT checklist](#) must be included with all submissions.

Clinical trial registration	<i>Provide the trial registration number from ClinicalTrials.gov or an equivalent agency.</i>
Study protocol	<i>Note where the full trial protocol can be accessed OR if not available, explain why.</i>
Data collection	<i>Describe the settings and locales of data collection, noting the time periods of recruitment and data collection.</i>
Outcomes	<i>Describe how you pre-defined primary and secondary outcome measures and how you assessed these measures.</i>

ChIP-seq

Data deposition

- Confirm that both raw and final processed data have been deposited in a public database such as [GEO](#).
- Confirm that you have deposited or provided access to graph files (e.g. BED files) for the called peaks.

Data access links
May remain private before publication. For "Initial submission" or "Revised version" documents, provide reviewer access links. For your "Final submission" document, provide a link to the deposited data.

Files in database submission
Provide a list of all files available in the database submission.

Genome browser session
(e.g. [UCSC](#))
Provide a link to an anonymized genome browser session for "Initial submission" and "Revised version" documents only, to enable peer review. Write "no longer applicable" for "Final submission" documents.

Methodology

Replicates
Describe the experimental replicates, specifying number, type and replicate agreement.

Sequencing depth
Describe the sequencing depth for each experiment, providing the total number of reads, uniquely mapped reads, length of reads and whether they were paired- or single-end.

Antibodies
Describe the antibodies used for the ChIP-seq experiments; as applicable, provide supplier name, catalog number, clone name, and lot number.

Peak calling parameters
Specify the command line program and parameters used for read mapping and peak calling, including the ChIP, control and index files used.

Data quality
Describe the methods used to ensure data quality in full detail, including how many peaks are at FDR 5% and above 5-fold enrichment.

Software
Describe the software used to collect and analyze the ChIP-seq data. For custom code that has been deposited into a community repository, provide accession details.

Flow Cytometry

Plots

Confirm that:

- The axis labels state the marker and fluorochrome used (e.g. CD4-FITC).
- The axis scales are clearly visible. Include numbers along axes only for bottom left plot of group (a 'group' is an analysis of identical markers).
- All plots are contour plots with outliers or pseudocolor plots.
- A numerical value for number of cells or percentage (with statistics) is provided.

Methodology

Sample preparation
Describe the sample preparation, detailing the biological source of the cells and any tissue processing steps used.

Instrument
Identify the instrument used for data collection, specifying make and model number.

Software
Describe the software used to collect and analyze the flow cytometry data. For custom code that has been deposited into a community repository, provide accession details.

Cell population abundance
Describe the abundance of the relevant cell populations within post-sort fractions, providing details on the purity of the samples and how it was determined.

Gating strategy
Describe the gating strategy used for all relevant experiments, specifying the preliminary FSC/SSC gates of the starting cell population, indicating where boundaries between "positive" and "negative" staining cell populations are defined.

- Tick this box to confirm that a figure exemplifying the gating strategy is provided in the Supplementary Information.

Magnetic resonance imaging

Experimental design

Design type
two even-related tasks: Monetary Incentive Delay Task (MID), Stop Signal Task (SST); one block design task: Emotional Face Task (EFT)

Design specifications
MID: The task consisted of 66 10-second trials. In each trial, participants were presented with one of three cue shapes (cue, 250 ms) denoting whether a target (white square) would subsequently appear on the left or right side of the screen and whether 0, 2 or 10 points could be won in that trial. After a variable delay (4,000-4,500 ms) of fixation on a white crosshair, participants were instructed to respond with left/right button-press as soon as the target appeared. Feedback on whether and how many points were won during the trial was presented for 1,450 ms after the response.
SST: The task was composed of Go trials and Stop trials. During Go trials (83%; 480 trials) participants were presented

with arrows pointing either to the left or to the right. During these trials, subjects were instructed to make a button response with their left or right index finger corresponding to the direction of the arrow. In the unpredictable Stop trials (17%; 80 trials), the arrows pointing left or right were followed (on average 300 ms later) by arrows pointing upwards; participants were instructed to inhibit their motor responses during these trials.

EFT: Participants watched 18-second blocks of either a face movie (depicting anger or neutrality) or a control stimulus. Each face movie showed black and white video clips (200-500ms) of male or female faces. Five blocks each of angry and neutral expressions were interleaved with nine blocks of the control stimulus. Each block contained eight trials of 6 face identities (3 female). The same identities were used for the angry and neutral blocks. The control stimuli were black and white concentric circles expanding and contracting at various speeds that roughly matched the contrast and motion characteristics of the face clips.

Behavioral performance measures

For both event related tasks MID and SST, performance tracking systems were implemented to adjust difficulty of the tasks to ensure the overall performance of each participant (i.e. successfully responded on ~66% of trials in the MID and 50% successful rate in inhibition trials in the SST). As a passive viewing task, there is no performance measure for the EFT.

Acquisition

Imaging type(s)

BOLD functional signal

Field strength

3 Tesla

Sequence & imaging parameters

Structural and functional MRI data were acquired at eight IMAGEN assessment sites with 3T MRI scanners of different manufacturers (Siemens, Philips, General Electric, Bruker). The scanning variables were specifically chosen to be compatible with all scanners. The same scanning protocol was used in all sites. In brief, high-resolution T1-weighted 3D structural images were acquired for anatomical localization and co-registration with the functional time-series. Blood-oxygen-level-dependent (BOLD) functional images were acquired with gradient-echo, echo-planar imaging (EPI) sequence. For all fMRI tasks, 300 volumes were acquired for each participant, and each volume consisted of 40 slices aligned to the anterior commissure/posterior commissure line (2.4 mm slice thickness, 1 mm gap). The echo-time (TE) was optimized (TE=30 ms, repetition time (TR)=2,200 ms) to provide reliable imaging of subcortical areas.

Area of acquisition

Whole brain scan

Diffusion MRI Used

Not used

Preprocessing

Preprocessing software

Functional MRI data were analysed with SPM8 (Statistical Parametric Mapping, <http://www.fil.ion.ucl.ac.uk/spm>). Spatial preprocessing included: slice time correction to adjust for time differences due to multi-slice imaging acquisition, realignment to the first volume in line, non-linearly warping to the MNI space (based on a custom EPI template (53x63x46 voxels) created out of an average of the mean images of 400 adolescents), resampling at a resolution of 3x3x3mm³ and smoothing with an isotropic Gaussian kernel of 5 mm full-width at half-maximum.

Normalization

see above

Normalization template

see above

Noise and artifact removal

At the first level of analysis, changes in the BOLD response for each subject were assessed by linear combinations at the individual subject level, for each experimental condition (e.g. reward anticipation high gain of Monetary Incentive Delay (MID) task), each trial was convolved with the hemodynamic response function to form regressors that account for potential noise variance, e.g. head movement, associated with the processing of reward anticipation. Estimated movement parameters were added to the design matrix in the form of 18 additional columns (three translations, three rotations, three quadratic and three cubic translations, and every three translations with a shift of ± 1 TR).

Volume censoring

N/A

Statistical modeling & inference

Model type and settings

At the first level of analysis, changes in the BOLD response for each subject were assessed by linear combinations at the individual subject level. For the second level analysis, we establish the following contrasts: For the MID anticipation phase we contrasted brain activation during 'anticipation of high win [here signaled by a circle] vs anticipation of no-win [here signaled by a triangle]'; For the emotional faces task (EFT) we contrasted brain activation during 'viewing Angry Face vs viewing Control [circles]'; For the stop signal task (SST) we contrasted brain activation during 'successful stop vs successful go'. The single-subject contrast images were then taken to the population-based weighted co-activation network analysis.

Effect(s) tested

For the activations of each contrast, the one-sample t-test was applied for each voxel.

Specify type of analysis: Whole brain ROI-based Both

Statistic type for inference
(See [Eklund et al. 2016](#))

Ridge-restricted canonical correlation analysis (RCCA) was applied to detect the overall correlation between fMRI clusters generated from WVCNA and internalising/externalising behaviours.

Correction

Either permutation or Bonferroni correction was applied wherever applicable.

Models & analysis

- n/a | Involved in the study
- Functional and/or effective connectivity
 - Graph analysis
 - Multivariate modeling or predictive analysis

Functional and/or effective connectivity

Report the measures of dependence used and the model details (e.g. Pearson correlation, partial correlation, mutual information).

Graph analysis

Weighted Voxel Co-activation Network Analysis (WVCNA) was applied to establish task specific segregations of highly activated voxels across the whole brain.

Multivariate modeling and predictive analysis

WVCNA and a further hierarchical clustering were applied to reduce the dimension of task fMRI data. The hence derived fMRI clusters were investigated for multivariate correlations with externalising and internalising behaviours through RCCA.